치의과학박사 학위논문

Effect of sonic hedgehog signal-modulating small molecules and insulin-like growth factor 1 on the generation of murine skin-derived precursors

Sonic hedgehog 신호조절 소분자물질 및 인슐린유사성장인자1이 마우스 피부유래전구세포 생성에 미치는 효과

2019년 2월

서울대학교 대학원

치의과학과 종양및발달생물학 전공

박 상 규

Effect of sonic hedgehog signal-modulating small molecules and insulin- like growth factor 1 on the generation of murine skin-derived precursors

지도교수: 노 상 호

이 논문을 치의과학 박사학위논문으로 제출함

2018년 10월

서울대학교대학원

치의과학과 종양및발달생물학 전공

박 상 규

박상규의 박사학위논문을 인준함

2018년 12월

위 원 장 _____ (인)

부 위 원 장 _____ (인)

위 원 _____ (인)

위 원 _____ (인)

위 원 _____ (인)

ABSTRACT

Effect of sonic hedgehog signal-modulating small molecules and insulin-like growth factor 1 on the generation of murine skin-derived precursors

Sangkyu Park

Department of Cancer and Developmental Biology

The Graduate School

Seoul National University

(Directed by Prof. Sangho Roh, D.V.M., Ph.D)

Stem cells have ability for self-renewal and to differentiate into various lineages. Multipotent stem cells are also known as adult stem cells or progenitor cells. They are limited regarding their lifespan and their differentiation capability is restricted to the tissue from which they originate compared with pluripotent stem cells. The skin has various type of adult stem cells. Skin-derived precursors (SKPs) have been widely investigated in recent years because of their multipotent differentiation ability and potential clinical

applications for various diseases. SKPs have the potential to differentiate various lineages such as adipogenic, osteogenic, chondrogenic and neural cells.

Neural crest cells are critical role in fetal development and keep their multipotent potential in several parts of the adult body. These cells can be isolated more easily from skin than from other tissues. SKPs exhibit many neural crest cell properties, and a number of their marker genes are also expressed in cultured SKPs. Recently, It has been presented that SKPs can act in the recovery of skin damage, wound closure and drug screening. However, the mechanisms involved in the generation of SKPs have not yet been clarified. Therefore, in this study, it has been investigated whether Shh signaling pathway affect self-renewal and proliferation of mSKP. The Shh signaling pathway is involved in the viability, proliferation, and differentiation of cells in embryonic development.

In this study, Shh signaling pathways was regulated in SKPs using small molecules and growth factors. Activation of Shh signaling pathway using Shh agonist, purmorphamine promoted proliferation and sphere formation of SKPs, whereas inhibition of Shh signaling pathway by a Shh antagonist, cyclopamine reduced proliferation and self-renewal of SKPs. In addition, a Gli inhibitor, GANT-1 also inhibited stemness property and generation of mSKPs. These data demonstrated that Shh signaling pathway is crucial to proliferation and self-renewal of mSKPs.

In addition, it has been investigated sphere formation, cell proliferation and antioxidant effect of insulin-like growth factor 1 (IGF1) in mSKPs. IGF1 have insulin-like structure. It is crucial to cellular function such as differentiation and cell proliferation, especially, having a role is increasing cell proliferation during early embryonic development. In this study, we demonstrated that IGF1 induces the expression of epithelial–mesenchymal transition markers and cell proliferation. It also increases the expression of anti-oxidative stress markers such as GPX1, HO-1 and Nrf2 in H_2O_2-treated mSKPs. These data suggest that IGF1 promotes the proliferation and sphere formation of mSKPs, and decreases oxidative stress of mSKPs *in vitro*.

Collectively, these studies provide the evidence for the roles and underlying mechanisms of Shh and IGF1 signaling pathway on proliferation and self-renewal during SKPs propagation. These data suggest that small molecules and IGF1 are important for basic research and therapeutic application in SKPs.

Keyword: Sonic hedgehog, Insulin-like growth factor 1, skin-derived precursor, small molecule, proliferation, self-renewal, stem cell

Student Number: 2007-23382

CONTENTS

LIST OF TABLES

LIST OF FIGURES

ABBREVIATIONS

shh	sonic hedgehog
IGF1	insulin-like growth factor 1
SKP	skin-derived precursor
MSC	mesenchymal stem cell
Smo	smoothened
NCC	neural crest cell
NCSC	neural crest stem cell
EMT	epithelial–mesenchymal transition
MET	mesenchymal-epithelial transition
Pur	purmorphamine
CP	cyclopamine
ROS	reactive oxygen species
GPX1	glutathione peroxidase 1
HO-1	heme oxygenase-1
Nrf2	nuclear factor erythroid 2–related factor 2

REVIEW OF LITERATURE

Skin-derived precursors

Skin is a complex of various component structures such as hair follicles, blood vessels, lipid and nerve. The skin stability depends on the ability of precursor cells for skin regeneration (Dai *et al*., 2018). For instance, epidermis part of the skin is regularly regenerated from epidermal stem cells. Studies of Toma et al. are based on hypothesis that the skin has population of precursors similar to neurospheres (Fernandes *et al*., 2008; Toma *et al*., 2001). The neurospheres constructing from neural stem cell by suspending culture protocol have been used to investigate neural precursor cells *in vitro* (Suslov *et al.*, 2002).

They first introduced the term skin-derived precursors (SKPs; Toma *et al*., 2001). These precursors derive from the dermis, and clones of individual single cells can proliferate and differentiate in culture to produce neurons, glia, smooth muscle cells and adipocytes in mice (Toma *et al.*, 2001).

These dermis-derived SKPs are distinct from mesenchymal stem cells (MSCs; Toma *et al.*, 2001). MSCs can be expanded *in vitro* while retaining their ability to differentiate into mesodermal lineage. MSCs exist in bone

marrow, adipose tissue, muscle and umbilical cord blood. Based on their morphology, self-renewal, differentiation potential, and surface markers many tissues have been identified as sources of MSCs (Alviano *et al.*, 2007; De Bari *et al.,* 2001; Erices *et al.,* 2000; Polisetty *et al.,* 2008). To confirm the differences between SKPs and MSCs, MSCs were cultured with SKP conditions (Hoogduijn *et al*., 2006). The MSCs were shown to survive, but they were difficult to proliferate and form spheres.

The human studies suggested that SKPs may be present within adult human skin. Thus, SKPs apparently proposed a novel multipotent adult stem cell. The ability to isolate and expand such a stem cell from an accessible, potentially autologous tissue source such as mammalian skin (Toma *et al.*, 2005). Fernandes and colleagues proposed that multipotent adult precursor cell in mammalian skin have characteristics similar to embryonic neural crest stem cells (NCSCs), including neural-crest-like differentiation potential *in vitro*. These precursors can be isolated, cultured and expanded as multipotent SKPs. In addition, they showed that dorsal skin hair follicle papilla contain neural-crest-derived cells, and SKPs generated from dorsal skin have neural-crest potential (Fernandes *et al*., 2004).

In addition, SKPs with neural crest properties have been cultured from murine, porcine and human skin (Hunt *et al.*, 2009). SKPs were isolated from skin and cultured on suspended state using modified neural stem cell medium containing epidermal growth factor (EGF), basic fibroblast growth factor

(bFGF) and B27 supplement (Toma *et al.*, 2001). This culture protocol confirmed the potential of the growth and expansion of spheres like neurospheres from skin (Hunt *et al.*, 2009). SKPs are able to form into spheres and are able to be subcultured serially (Fig. 1). The murine SKPs can be passaged for 5 months (Toma *et al*., 2001) and the human SKPs passaged for over 1 year are capable of preserving normal karyotype (Toma *et al*., 2005). Porcine SKPs also presented similar in vitro culture properties with that of mouse and human (Dyce *et al*., 2004). These results illustrate the self-renewal capacity of SKPs, and their the potential to differentiate into mesodermal and neural lineages. Furthermore, SKPs express various markers including Nestin, a neural stem cell marker, similar to precursor cell populations (Dai *et al.*, 2018). Primary SKP spheres and passaged spheres also express the extracellular matrix proteins fibronectin and vimentin (Fernandes *et al*., 2004; Toma *et al*., 2001). In addition, SKPs express the various transcription factors such as Snail, Twist Dermo-1, SHOX2 and Sox9, which are also expressed in neural crest cells (Fernandes *et al*., 2004; Fernandes *et al*., 2008).

SKPs include populations of neural crest cells. SKPs and neural crest cells also have similar differential ability to differentiated into various lineages such as neurons, Schwann cells, adipocytes and smooth muscle cells (Fernandes *et al.*, 2008; Fernandes *et al.*, 2009). SKPs were antigenically distinct from epidermal, melanocytic and MSCs populations (Biernaskie *et al.*, 2006; Dai *et al.*, 2018; Toma *et al.*, 2001). SKPs were shown to be similar to

neural stem cells in their profile and cultivated shapes. However, they expressed some of mesodermal set of markers (Fernandes *et al.*, 2008).

The mesoderm has various structures and cell lineages such as adipocytes, myocyte, osteocyte and chondrocyte. SKPs are capable of differentiation into the mesodermal lineage without growth factors with fetal bovine serum (Toma *et al.*, 2001).. The differentiated cells from SKPs demonstrate presence of adipogenic and osetogenic markers. The murine SKP-derived adipocytes contain lipid vesicles that are stained by oil-red-O (Toma *et al.*, 2001).

Therefore, SKP also have the ability to differentiate into functional neuronal and glial cells from skin (Fernandes *et al.*, 2009). The neuronal differentiation of SKPs has been successfully repeated by a number of groups in mouse (Gingras *et al.*, 2007), pig (Dyce *et al.*, 2004) and human (Hunt *et al.*, 2008, Toma *et al.*, 2005). The efficiency of neuronal differentiation is low as only a small population (3-7%) of SKPs can differentiate neurons under neuronal culture medium (Toma *et al.*, 2001).

In addition, they are able to differentiate into Schwann cell like in the presence of forskolin and neuregulin-1β without serum (Biernaskie *et al.*, 2006; McKenzie *et al.*, 2006). The murine SKPs can generate cells positive for S100β, GFAP, p75NTR and the myelin proteins MBP. As a result, SKPs showed that 83% of SKPs differentiate into Schwann-like cells in under forskolin and

neuregulin-β in mouse and human (Biernaskie *et al*., 2006; McKenzie *et al*., 2006).

SKPs can be isolated from the dermis. The dermis has variety of structure. Therefore, location of SKPs has a question. First, the cells expressing SKP markers are different from the epidermal stem cells of bulge (Fernandes *et al*., 2004). However, whisker vibrissal papillae express Snail, Twist, Versican, Nexin and Wnt5a in the late stages of embryonic development (Fernandes *et al*., 2004). Therefore, the SKPs originate from the papillae in hair follicle or vibrissal. SKPs are also positive for papilla-related markers Nexin, Versican and Wnt5a (Fernandes *et al*., 2004). Whisker vibrissal papilla cultured under same condition form sphere similar to SKPs (Fernandes *et al*., 2004). Similar results were showed from rat whisker papilla and human facial hair (Hunt *et al*., 2008).

In addition, formed spheres from whisker papilla differentiated into neuronal cells (Fernandes *et al*., 2004; Hunt *et al*., 2008). They could also be differentiated into Schwann cells (Hunt *et al*., 2008). These results suggest that niche for SKPs is the hair follicle papilla. On the other hand, the origin of the SKPs found in back skin remains to be determined. The dermal papillae in the back skin are derived from a different embryonic origin. Interestingly, other populations of cells associated with the hair follicle were reported to originate from the neural crest and to form SKP-like spheres *in vitro* (Wong *et al*., 2006). However, these cells were positive for p75NTR and Sox10, two markers that

are not expressed in facial SKPs (Fernandes *et al*., 2004; Wong *et al*., 2006). Therefore, the identity of the cell of origin for back skin-derived SKPs remained an open question until very recently.

The some of SKPs capacity is to self-renew and differentiate into mesodermal lineage. However, SKPs and MSCs constitute distinct cell populations. Other precursors and stem cells have been confirmed from various research. In the study of Toma and colleagues, vimentin and fibronectin were expressed in MSCs by immunofluorescence staining but MSCs were negative for nestin (Toma *et al*., 2001). In contrast, SKPs were positive for Nestin and Fibronectin but negative for cytokeratin. SKPs were also observed to be smaller and less flattened than MSCs. When MSCs were cultured under SKPs conditions, the MSCs were found to survive, but did not proliferate or form floating spheres. These results support SKPs and MSCs are different from one another.

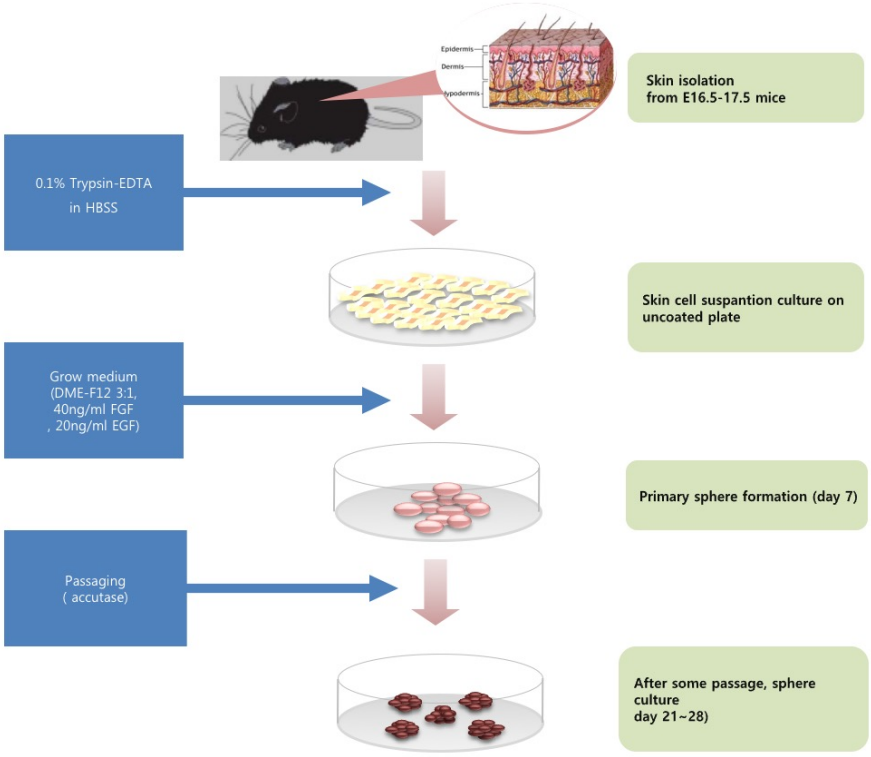

Figure 1. Procedure of isolation of the skin-derived precursors

Small molecules

Small molecules are low molecular weight molecules that include lipids, monosaccharides, other natural products and metabolites, as well as drugs. Small molecules are increasingly being used as tools to interrogate cellular signaling pathways. In particular, the molecules especially affect stem cell property by regulating, self-renewal and differentiation/de-differentiation. Small molecules are being used widely to decipher the key regulatory pathways in stem cell biology (Schmole *et al.*, 2013).

Small molecules or other agonists of stemness-related pathways can be used in the generation of pluripotent stem cells (Li *et al.*, 2009; Huangfu *et al.*, 2008a). By reprogramming critical factors or enhancing the reprogramming efficiency. G9a histone methyltransferase inhibitor BIX- 01294 was identified to be involved reprogramming with reprogramming factors, and it found to increases the reprogramming efficiency of Oct4 and Klf4-infected NPCs up to around 8-fold. BayK 8644, an L-type calcium channel antagonist, enhances reprogramming efficiency of mouse embryonic fibroblasts (MEFs) when combined with BIX-01294 (Shi *et al.*, 2008).

In addition, various inhibitors and activators of GSK-3 influenced the self-renewal of embryonic stem (ES) cells. The activation of canonical Wnt signaling via 6-bromoindirubin-3′-oxime (BIO) activates the transcription of

Oct3/4, Rex-1 and Nanog which are involved in the maintenance of a pluripotent, undifferentiated state in human and mouse ES cells (Li *et al.*, 2009). In addition, Wnt pathway influences on self-renewal of pluripotent stem cells (Sato *et al.*, 2004). A BIO-mediated activation of Wnt signaling was reversed by withdrawal of BIO resulting in differentiation of human and mouse ES cells.

Self-renewal

Self-renewal is proliferation with maintenance of the undifferentiated state (Ying *et al.*, 2008). Maintaining self-renewal capabilities is essential for stem cell cultivation (Ying *et al.*, 2008). ES cells need to be cultured on feeder cell layer or coating molecules for maintenance of stemness and self-renewal (Beattie *et al.*, 2005). Self-renewal involves stemness-related genes, signaling pathway and cell-extrinsic signals from the niche and the microenvironment (Greber *et al.*, 2007). The self-renewal process is controlled differently in mouse and human ES cells. Self-renewal depends on bFGF and Transforming growth factor beta/Activin/Nodal signaling pathways in human ES cells, while it is regulated by bone morphogenic protein and Leukemia inhibitory factor signaling pathway in mouse ES cells (Levenstein *et al.*, 2006; Niwa *et al.*, 1998; Xiao *et al.*, 2006). The reduction of stem cell property decreases self-renewal.

This event can cause weakened stem cell function and regenerative capacity. On the other hands, cancers arising from mutations inappropriately activate self-renewal programs.

MSCs also have the ability to self-renew and differentiate. MSCs are important for tissue maintenance and repair (Mahmood *et al.*, 2010). Unlike ES cells, MSCs maintained balance specialization between differentiation for regeneration and retention of stem cell in the body. This balance is regulated by the microenvironment and niche (Schmole *et al.*, 2013). SKPs are also self-renewing multipotent stem cells that reflect an *in vitro* correlate of neural stem cells when grown in substrate free conditions (Toma *et al*., 2001).

Sonic hedgehog signaling

The Hedgehog (Hh)-Gli signaling pathway is critical roles in embryonic development, stem cells, and various precursor cells (Bermudez *et al.*, 2013; Fu *et al.*, 2004; Lai *et al.*, 2003). Hh ligands attach at a Patched, cell-surface receptor. Its action releases inhibition of Smoothened (Smo). Smo activates the canonical Hh pathway through the Gli-dependent transcription (Arnhold *et al.*, 2016). The Hh signaling pathway also plays a critical role in

endoderm and mesoderm development during embryogenesis (Fernandes-Silva *et al.*, 2017).

Recent reports also show that Hh-Gli signaling pathway controls the self-renewal of neural stem cells by regulating Nanog, p53 and Foxm1 (Besharat *et al.*, 2018). Foxm1 in neural stem cell is controlled by Gli1 and Gli2, directly but also indirectly via their modulation of the expression of Nanog, which was shown to transcriptionally activate Foxm1 (Besharat *et al.*, 2018). Sonic hedgehog (Shh) knock-out mice are embryonic lethal because these mice have developmental defects from inappropriate patterning vertebrate embryonic tissues (including the brain, spinal cord, and axial skeleton; Liu *et al.*, 2014; Stanton *et al.*, 2009).

In vertebrate embryos, enteric neural crest cells (NCCs) from the vagal level of the neural tube provide the enteric nervous system. These cells enter the foregut and then colonize the entire gut in a rostro-caudal wave. The gut endoderm-derived Shh and mesenchyme-derived factors act together to orchestrate the development and the concentric organization of NCCs and musculature of developing gut. Furthermore, NCCs can be maintained in culture without losing stem cell properties in the presence of Shh.

Calloni and colleagues suggested that the recombinant Shh increases the proliferation of cephalic NCCs progenitors both mesenchymal and neural lineages and enhances the development of such precursors from the trunk NCCs. Shh especially decreases the neural-restricted precursors without affecting the

overall cephalic NCC survival and proliferation. On the other hands, Shh improved on mesenchymal precursors by multipotent cephalic NCCs (Calloni *et al*., 2007).

The Shh signaling pathway plays an important role in embryonic development and has rapidly emerged as one of the most important regulators of oncogenic transformation. The Patched also negatively interacts with a putative G- protein coupled receptor like Smo. Upon association of Patched with its ligand Shh, the inhibition of Smo is relieved resulting in up-regulation of a number of target genes, such as Wnt, genes of the TGF-β families and Patched itself. Inactivation of Patched by mutations therefore results in the constitutive activation of Smo, which is characterized by over-expression of Gli1, ending in uncontrolled cell proliferation (Fu *et al*., 2004).

Recent studies have suggested that Shh promotes ES cell proliferation via Gli family activation in mice (Wu *et al.*, 2010). The Hh signaling pathway also regulates the self-renewal of mammary stem cells via Bmi1, a Polycomb group protein (Liu *et al.*, 2011; Memmi *et al.*, 2015). Bmi1 participates in brain development and stem cell proliferation.

Epithelial–mesenchymal transition

The phenomenon that epithelial cells acquire mesenchymal traits, termed as epithelial–mesenchymal transition (EMT), has been observed in physiological and pathological processes, including embryogenesis (Gros *et al.* 2014; Yoshino *et al.*, 2014), inflammation (Correa-Costa *et al.*, 2014), fibrosis (Grande *et al.*, 2015; Schneider *et al.*, 2012), wound healing (Banerjee *et al.*, 2015), and cancer progression (Wei *et al.*, 2015).

EMT plays a critical role in the cancer cells (Sato *et al.*, 2016). The EMT is a reversible process which polarized epithelial cells change to characteristics of mesenchymal cells by their polarity losing (Chen *et al.*, 2017). Changed cells had migratory activity and promoted production of extracellular matrix (ECM) components (Wei *et al.*, 2015).

EMT acts critical roles that develop embryogenesis and give rise to mesoderm and move shift neural crest cells. EMT-related gene expressions are changed by classic EMT-inducing factors such as N-cadherin, Snail, Slug, Twist, ZEB1, and ZEB2. EMT promotes metastasis and stem cell-like property in cancer cells (Valastyan *et al.*, 2011).

INTRODUCTION

SKPs exist in fetal, neonatal, and adult skin. SKPs are multipotent stem cells which contain various stem cell populations, including NCSCs (Biernaskie *et al.*, 2006; Fernandes *et al.*, 2008; Fernandes *et al.*, 2009). SKPs have the potential to differentiate along various lineages. They can become adipogenic, osteogenic, and chondrogenic cells. They can also become neural cells such as neurons, glial cells, and Schwann cells (Biernaskie *et al.*, 2006; Fernandes *et al.*, 2008; Fernandes *et al.*, 2009; Mao *et al.*, 2015). It has recently been shown that SKPs can act in the recovery of skin damage, in wound healing, and in the regeneration of hair follicles (Su *et al.*, 2009).

NCSCs persist through fetal development and keep their multipotency in various parts of the body. These cells can be isolated more easily from skin than from other tissues (Dupin *et al.*, 2012; Su *et al.*, 2009). SKPs exhibit many neural crest cell properties, and a number of marker genes for primitive embryonic NCSCs are also expressed in cultured SKPs (Fernandes *et al.*, 2008; Shi *et al.*, 2013). In addition, SKPs behavior is similar to that of NCSCs when transplanted into the neural crest migratory stream of embryonic chicks (Fernandes *et al.*, 2008). Although the isolation and culture of SKPs has been reported in many species including human, rat, mouse, and pig (Fernandes *et al.*, 2009; Naska *et al.*, 2016; Suflita *et al.*, 2013; Zhao *et al.*, 2010), the critical

signaling pathways for cell property maintenance, self-renewal, and proliferation are unclear. Stem cells generally have two signatures: self-renewal and differentiation potency. These two features in SKPs are regulated by intrinsic and extrinsic signals from various niches (Dupin *et al.*, 2012). Sphere-type SKPs are generated using a suspension culture system. Dissociated single cells from primary spheres form secondary spheres expressing the SKP markers. Various studies have reported that SKPs can be obtained using 3D colony-forming systems such as methylcellulose or Matrigel, where the clonality of the spheres can also be confirmed (Biernaskie *et al.*, 2006; Fernandes *et al.*, 2009; Liu *et al.*, 2011).

The Hh-Gli signaling pathway participates in brain development, self-renewal of neural stem cells, and proliferation of various precursor cells (Bermudez *et al.*, 2013; Fu *et al.*, 2004; Lai *et al.*, 2003). Recent reports also show that Hh-Gli signaling pathway controls the self-renewal of neural stem cells by regulating Nanog, p53 and Foxm1 (Besharat *et al.*, 2018). Hh ligands bind to a cell-surface receptor called Patched. The binding relieves its inhibition of Smo and allows the signaling pathway to proceed. Smo activates the canonical Hh pathway through the Gli-dependent transcription of multiple targets, including N-myc, cyclin D, Patched, Gli1, and Gli2 (Arnhold *et al.*, 2016). Furthermore, the Hh signaling pathway plays a critical role in endoderm and mesoderm development during embryogenesis (Fernandes-Silva *et al.*, 2017). Shh knock-out mice are embryonic lethal because these mice have

problems patterning vertebrate embryonic tissues including the brain, spinal cord, and axial skeleton (Liu *et al.*, 2014; Stanton *et al.*, 2009).

Recent studies have demonstrated that Shh stimulates ES cell proliferation via Gli family activation and protein kinase C cooperation in mice (Wu *et al.*, 2010). The Hh signaling pathway also regulates the self-renewal of mammary stem cells via Bmi1, a Polycomb group protein (Liu *et al.*, 2011; Memmi *et al.*, 2015). Bmi1 participates in brain development and stem cell proliferation. It is also able to replace some reprogramming factors such as Sox2, Klf4, and N-myc when induced pluripotent stem (iPS) cells are generated from murine embryonic fibroblasts (Kang *et al.*, 2014; Moon *et al.*, 2008). Synthetic or natural small molecules are widely used to understand and regulate stem cells. Small molecules such as Purmorphamine (Pur) and oxysterol activate the Shh signaling pathway. They are able to replace Bmi1 to generate iPS cells. They also induce Bmi1, Sox2, and N-myc expression to promote the proliferation of neural precursor cells (Kang *et al.*, 2014).

Both the EMT and the mesenchymal-epithelial transition (MET) play important roles in embryonic development, fibrosis, and cancer progression (Islam *et al.*, 2016; Zhang *et al.*, 2016; Zhang *et al.*, 2015). The EMT influences organ and tissue formation during embryogenesis, including the neural crest, heart, nervous system, and craniofacial structure (Zhang *et al.*, 2016). More recently, the effect of the EMT on the self-renewal and stemness of cancer stem cells (stem-like cells in tumors) was studied (Cochrane *et al.*, 2015). The EMT

is characterized by cells losing their epithelial state and acquiring fibroblast-like properties. Cells produced by the EMT show decreased intercellular adhesion and elevated motility (Memmi *et al.*, 2015). Specifically, they show decreased expression of E-cadherin and increased expression of mesenchymal cell markers such as N-cadherin, fibronectin, α-smooth muscle actin (α-SMA) and vimentin (Fu *et al.*, 2013; Islam *et al.*, 2016; Williamson *et al.*, 2016). In the present first study, the effects of the Shh signaling pathway on the generation and propagation of murine SKPs (mSKPs) were investigated. The mSKP were also explored whether activation of the Shh signaling pathway contributes to the their self-renewal and proliferation. The sphere formation of SKPs in suspension culture revealed a correlation between the EMT and the Shh signaling pathway. This study highlights the fact that the Shh pathway is important to the self-renewal and cell proliferation of SKPs.

Insulin-like growth factor 1 (IGF1) plays a critical role in the regulation of cellular growth and proliferation, and inhibited IGF1 signaling results in growth delay (Wang *et al.*, 2018). It is composed as 70 amino acid polypeptides and have insulin-like structure. Previous studies have also shown that IGF1 can increase the total cell number in early embryonic development delay (Wang *et al.*, 2018). IGF1, which is binding at IGF receptor tyrosine kinase receptor, acts as survival factor and blocks cell apoptosis in various cell types. IGF1 treatment has sustaining growth and resisting apoptosis of cancer cell (Yao *et al.*, 2016).

ROS are particularly generated as products of mitochondrial respiration or are produced by oxidases like nicotine adenine diphosphate (NADPH) oxidase and xanthine oxidase (Baregamian *et al.*, 2012; Higashi *et al.*, 2010). ROS production is the major mechanism relating cytotoxicity to normal cells. Many studies have suggested that antioxidants have a protective effect on chemical-induced cytotoxicity. Hydrogen peroxide (H_2O_2) is a typical inducer of oxidative stress, which causes cellular dysfunction, cell damage, and vascular disease. H_2O_2 can also induce cellular senescence and apoptosis (Kim *et al.*, 2017; Park, 2013).

Various cells are promoted release of unknown molecules by IGF1 under oxidative stress. It protects dopamine neurons against oxidative stress (Ayadi *et al.*, 2016). IGF1 also enhances endothelial antioxidant activity, primarily via upregulation of glutathione peroxidase-1 (GPX1) expression and activity (Wang *et al.*, 2018; Huat *et al.*, 2014). Furthermore, potential of antioxidant effects have by IGF1 in human aortic endothelial cells (Garcia-Fernandez *et al.*, 2005; Higashi *et al.*, 2010). It also contributes to the survival of various stem cells (Huat *et al.*, 2014; Tseropoulos *et al.*, 2018; Yao *et al.*, 2016). IGF signaling is closely related to the growth and proliferation of cancer stem-like cells (Yao *et al.*, 2016). In addition, IGF1 prevents senescence and reduces vascular problem by oxidant stress (Garcia-Fernandez *et al.*, 2005; Higashi *et al.*, 2010). However, the role of IGF1 in SKPs is not fully elucidated.

Several studies have shown that IGF signaling is related to EMT phenotype in mammary cells (Yao *et al.*, 2016). The overexpressing IGF1R acquire depolarization and EMT phenotype following IGF1 stimulation in breast cancer cells (Chen *et al.*, 2017). The overexpression of active IGF1R also induces EMT phenotype and anchorage-independent proliferation in vivo in breast cancer (Baregamian *et al.*, 2012). In addition, IGF signaling pathway is important role on the improvement of EMT phenotype and maintaining stemness of cancer stem cells in lung cancer (Yao *et al.*, 2016). However, the precise mechanisms involved in the role of IGF signaling in EMT are unclear in SKPs. In the second study, the effects of the IGF1 signaling pathway on the generation and propagation of mSKPs were investigated. The sphere formation of SKPs in suspension culture revealed a correlation between the EMT and the IGF1 signaling pathway. The mSKPs were also explored whether IGF1 have an antioxidant effect under H_2O_2-mediated and aged state. This study highlights the fact that the IGF1 treatment promotes the proliferation of SKPs and has antioxidant effect in H_2O_2-mediated damaged SKPs.

MATERIALS AND METHODS

Animals

A total of 90 pregnant ICR female mice (DBL, Chungbuk, Korea) were used in studies (8 to 15 mice per group). Six to fifteen embryos could be obtained from each pregnant female. All animal experiments were performed under the guidelines of the Institutional Animal Care and Use Committee of Seoul National University (approval number: SNU-131231-4).

Chemicals

All inorganic and organic compounds were obtained from Sigma-Aldrich (St. Louis, MO, USA). All liquid solutions were purchased from Thermo Fisher Scientific (Waltham, MA, USA) unless otherwise stated.

Propagation and isolation of mSKPs

The mSKPs were isolated by previously described protocols, with a few modifications (Fig. 1; Fernandes *et al.*, 2009; Park *et al.*, 2018). Back skin obtained from E16.5-17.5 mouse embryos was washed 3 times in phosphate-buffered saline (PBS; WelGENE, Daegu, Korea) with 3X penicillin/streptomycin (Gibco, Grand Island, NY, USA), and then minced into

small pieces using a blade. Small pieces of back skin were incubated for 40 min in a 37°C, 5% CO_2 cell culture incubator on a 60 mm culture dish containing 4 ml of 0.05% (w/v) trypsin solution (Gibco) or 1X TryPLE^{TM} (Gibco). The incubated skin pieces were pipetted up and down 30 times for single cell dissociation. Dulbecco's modified Eagle medium (DMEM; WelGENE) with 10% fetal bovine serum (FBS; Atlas Biologicals, Fort Collins, CO, USA) was added onto the incubated skin pieces and dissociated single cells for enzyme neutralization. Skin and cell suspensions were strained through 100 μm and 40 μm nylon cell strainers (BD, Franklin Lakes, NJ, USA) for single cell isolation. Strained single cells were centrifuged at 250 X *g* for 4 min. The cell pellet was re-suspended in 5 ml of SKPs medium including DMEM/F-12 (3:1 mixture, v/v, Gibco), 2% B27 supplement (B27; Gibco), 20 ng/ml EGF (Peprotech, Rocky Hill, NJ, USA), and 40 ng/ml bFGF (Peprotech). The single cells were counted and then cultured in a 90 mm Petri dish in a 37°C with 5% CO_2 atmosphere. Fresh SKP medium was replaced every 3 days. The cells were passaged every 5-7 days. The formed spheres were single-cell dissociated by pipetting with Accutase^{TM} (Gibco).

Differentiation of mSKPs into various lineages

For differentiation, spheres were centrifuged in basal SKP medium without growth factors. The spheres were dissociated using the same methods

as in subculture. Dissociated single cells or spheres were seeded on the coated plate. For adipocyte differentiation, seeded SKPs were treated with DMEM／F12 containing 10% FBS, 1 mM dexamethasone (Sigma), 1 mM isobutylmethylxanthine (Sigma), and 20 μg/ml insulin (Sigma). For osteogenic differentiation, seeded SKPs were treated with αMEM (Gibco) including 10% FBS, 0.1 μM dexamethasone (Sigma), 2 mM ascorbic acid (Sigma), and 10 mM Glycerol 2-Phosphate (Sigma). For staining, differentiated cells were fixed with 4% formaldehyde at 4℃ for 1 h, and then washed twice with PBS. The cells were then stained with Oil-red O or Arizarin Red S. For neural differentiation, mSKPs were attached on laminin- and poly D-lysine-coated 6-well plates (BD). Cells were incubated in neurobasal medium™ (Gibco), including B27 and 0.5 mM dibutyryl cAMP (Peprotech), for 14 days.

Immunofluorescence staining

Immunofluorescence staining was performed according to standard protocols. Briefly, mSKPs or differentiated cells from mSKPs were fixed in 4% paraformaldehyde, permeabilized with 0.25% Triton X-100 (Sigma), and blocked with 1% goat serum in PBS. The fixed cells were stained with the indicated antibodies against table 1. The treated cells were covered with SlowFade antifade reagent with DAPI (SlowFade™ Gold antifade with DAPI) for nuclear staining, and covered with a glass coverslip. Images were captured

with confocal microscopes (LSM800, Carl Zeiss, Oberkochen, Germany; FV-300, Olympus, Tokyo, Japan).

Table 1. Antibodies and dilutions for immunofluorescence analysis

Antibody	Dilution	Catalog Number	Company
PAX6	1:50	PA1-801	Thermo Fisher Scientific, Waltham, MA, USA
NGFR (p75NTR)	1:500	AB1554	Millipore, Darmstadt, Germany
MBP	1:100	sc-13912	Santacruz, Dallas, TX, USA
S100b	1:100	sc-7852	Santacruz
α-Sma	1:500	ab32575	Abcam, Cambridge, UK
Chd2 (N-cad)	1:100	NBP1-48309	Novus Biologicals, Littleton, CO, USA
Anti-mouse IgG-FITC	1:1000	A-11029	Thermo Fisher Scientific
Anti-rabbit IgG-FITC	1:500	AP132F	Millipore
Anti-goat IgG-FITC	1:500	A-11055	Thermo Fisher Scientific

Reverse transcription (RT)-PCR

For total RNA isolation from sphere-forming mSKPs, I followed the commercial protocol of the Ambion PureLink™ RNA Mini Kit (Thermo Fisher Scientific). For the synthesis of first-strand cDNA, reverse transcription was performed for 1 h at 42°C in a final reaction volume of 25 μl using cDNA synthesis kit (Thermo Fisher Scientific). Synthetic cDNA from the RNA of mSKPs and differentiated cells was used for each PCR reaction. Each reaction contained 50 ng cDNA, 20 pmol each of specific primers, and AccuPower™ PCR Premix (Bioneer, Daejeon, Korea). Thermal cycle was repeated 34 times.

Real-time quantitative PCR

The cDNA was analyzed using real-time quantitative PCR (qPCR). For optimal quantification, primers were designed using Primer Express software (Applied Biosystems). The qPCR reactions were performed using the ABI PRISM 7500 system and SYBR™ Premix Ex Taq II (Takara Bio Inc., Shiga, Japan). All samples were run in triplicate as technical replicates. The following amplification procedure was employed. Data were analyzed using the 7500 System Sequence Detection software (Applied Biosystems). All samples had the same starting quantities of all candidate reference genes, based on the standard curves generated for those genes. All procedures and data analyses followed MIQE guidelines. The specific primer sequences targeting

genes for stemness, differentiation, EMT, Shh signaling and the neural crest are listed in Table 2.

Table 2. Primer sequences for qPCR analysis

Gene		Primer Sequence (5' to 3')	Accession
CD49f	Forward	GATGCTGCCAACGCTGTATTC	NM_001277970
	Reverse	GCCGTTCTGGCAACAGATG	
c-Myc	Forward	TGCGGTCGCTACGTCCTT	NM_010849
	Reverse	TCCAAGTAACTCGGTCATCATCTC	
Oct4	Forward	CCGTGTGAGGTGGAGTCTGGAG	NM_013633
	Reverse	GCGATGTGAGTGATCTGCTGTAGG	
Ngfr	Forward	CAGGGAAACATCTGGAAACGA	NM_033217
	Reverse	TGGACCAGGTTTTGAACAGACA	
Smo	Forward	AAGGCCACCCTGCTCATCTG	NM_176996
	Reverse	AGGCCTTGGCGATCATCTTG	
Nanog	Forward	AGGACAGGTTTCAGAAGCAGAAGT	NM_028016
	Reverse	TCAGACCATTGCTAGTCTTCAACC	
Klf4	Forward	ACTATGCAGGCTGTGGCAAAA	NM_01063
	Reverse	CCGTCCCAGTCACAGTGGTA	
Bmi1	Forward	CGCTCTTTCCGGGATCTTTT	NM_007552
	Reverse	CCCTCCACACAGGACACACA	
Twist	Forward	AGAAGAGCAGAGACCAAATTCACA	NM_011658
	Reverse	GCTGCCCCTCTGGGAATC	
Nestin	Forward	GGCATCCCTGAATTACCCAA	NM_016701
	Reverse	AGCTCATGGGCATCTGTCAA	
Lsd1	Forward	GTTCATCAGGAATCGCACATTG	NM_001347221
	Reverse	GCTGTTGTAAGGCGCTTCCA	
Sox9	Forward	GCAGACCAGTACCCGCATCT	NM_011448
	Reverse	CCTCCACGAAGGGTCTCTTCT	
Patched1	Forward	CGAGACAAGCCCATCGACATTA	NM_001328514
	Reverse	AGGGTCGTTGCTGACCCAAG	
Cdh2	Forward	AGCGCAGTCTTACCGAAGG	NM_007664
	Reverse	TCGCTGCTTTCATACTGAACTTT	
Fn1	Forward	GATGTCCGAACAGCTATTTACCA	NM_001276408
	Reverse	CCTTGCGACTTCAGCCACT	
Vim	Forward	CGTCCACACGCACCTACAG	NM_011701
	Reverse	GGGGGATGAGGAATAGAGGCT	
Tgfb1	Forward	CTCCCGTGGCTTCTAGTGC	NM_011577
	Reverse	GCCTTAGTTTGGACAGGATCTG	
a-Sma	Forward	GTC CCA GAC ATC AGG GAG TAA	NM_007392
	Reverse	TCG GAT ACT TCA GCG TCA GGA	
Gapdh	Forward	AGGTCGGTGTGAACGGATTTG	NM_001289726
	Reverse	TGTAGACCATGTAGTTGAGGTCA	

Western blot analysis

The mSKPs receiving various treatments were centrifuged and collected. Collected mSKPs were lysed by Passive lysis buffer (Promega, Madison, WI, USA). Protein was quantified using the Pierce BCA protein assay kit (Thermo Fisher Scientific). Equal amounts of protein (30-50 μg) from each treated group were analyzed on a 12% sodium dodecyl sulfate polyacrylamide gel. After transfer to a nitrocellulose membrane, the membrane was incubated with primary and secondary antibodies on a shaker. Detection was performed using WesternBright^{TM} Quantum (Advansta, Menlo Park, CA, USA), according to the manufacturer's recommended protocol. Western blot data were analyzed using the GeneGnome XRQ System (Syngene, Cambridge, UK).

Cell proliferation assay

The mSKPs were measured for cell proliferation using the WST-1 cell proliferation assay (Daeil Lab Service, Seoul, Korea), following the manufacturer's instructions. Briefly, mSKP spheres were harvested by centrifugation. The mSKPs were dissociated to single cells by accutase. Dissociated cells were serially diluted and then plated on 96-well plates in SKP medium. Each plate was analyzed by a macro-well reader at an absorbance of 450 nm, after plated cells had been cultured for 48 to 72 h.

Apoptosis analysis by Annexin V assay using flow cytometry

The mSKPs were plated at a density of 1.5×10^5 cells/ml. Cultured suspension cells were treated with the small molecules Pur (Shh agonist), cyclopamine (CP; Shh antagonist), and/or GANT-61 (Gli antagnonist) for 72 h. Cells were stained with an Annexin V assay kit (Cayman, Ann Arbor, MI, USA) according to the manufacturer's protocol. Briefly, SKPs were dissociated by accutase and then washed twice in cold PBS. Cells were resuspended in binding buffer, and 10 ml of FITC-conjugated Annexin V was added. Propidium iodide or 7-Aminoactinomycin D were also added to detect nonviable cells. Dissociated cells were incubated for 15 min in the dark, and an additional 400 μl of binding buffer was added. The cells were analyzed within 1 h by flow cytometry. Acquisition was performed on a FACS Calibur instrument using CellQuest Pro software (BD). Each analysis was performed on at least 10,000 events.

Measurement of ROS

A DCF-DA cellular ROS detection assay (Abcam, Cambridge, MA, USA) was used to measure hydroxyl, peroxyl, and other ROS activity within cells. A total of 2×10^4 cells per well were seeded on a 96-well plate and allowed to culture for 24 h. The suspended cells were then stained with 25 μM DCF-DA for 45 min at 37°C. Cells were then treated with H_2O_2 and/or IGF1 for 24

h. Finally, fluorescent intensity was determined by fluorescence spectroscopy with excitation and emission spectra of 485 and 535nm, respectively.

Statistical analysis

All numerical values in this study are expressed as the mean ± SD. Statistical analyses were performed using a two-tailed student's *t*-test for comparison between two groups, or a one-way ANOVA for the comparison of three or more groups. Differences were considered statistically significant at p values < 0.05.

RESULTS

Isolation, culture, and characterization of mSKPs from murine fetal back skin

The mSKPs formed spheres from single cells in suspension culture (Fig. 2A). After 5-7 d the spheres grew larger, and some spheres began to aggregate. The mSKPs proliferated, expanded, and reformed spheres after subculture via accutase and pipetting (Fig. 2B, C). They were expressed neural markers such as Nestin, NGFR and HNK1 (Fig. 2D). After 3-4 weeks of neural differentiation induction, neural cells were identified by immunofluorescence analysis using neural cell markers that are only expressed in differentiated cells, such as NGFR, MBP, S100b, and PAX6 (Fig. 2E-H). The mSKP spheres also differentiated into adipogenic cells (Fig. 2I). The differentiated adipogenic cells were confirmed by Oil-Red O (Fig. 2J). In addition, mSKPs were differentiated into osteogenic cells and these cells were positive Alizarin Red S (Fig. 2K). These results demonstrate that cell spheres isolated from murine back skin have SKP properties.

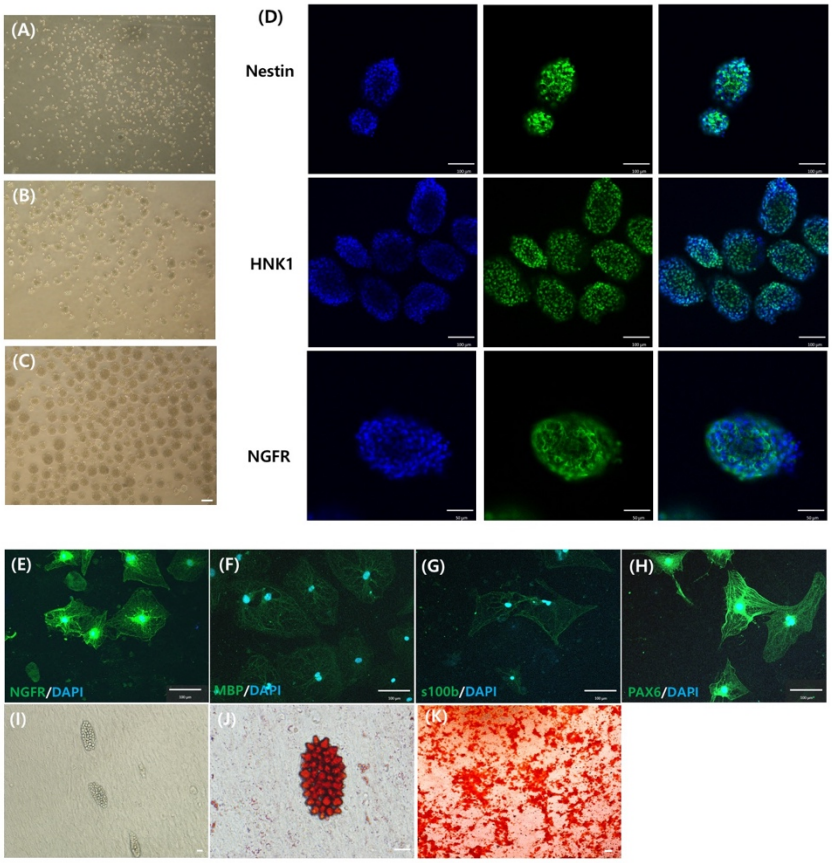

Figure 2. Isolation and differentiation of murine skin-derived precursors (mSKPs). (A) Single cells were separated from the back skin of murine fetuses. (B) Primary spheres were generated from isolated single cells. (C) Secondary spheres were larger and more condensed than primary spheres. The mSKPs were stained with neural markers (green) such as Nestin, human natural killer-1 (HNK1) and nerve growth factor receptor (NGFR). DAPI (blue) is shown in merged images. (E-H) The mSKPs were differentiated into Schwann cells on PDL and laminin-coated dishes from d 14 to 21, using Schwann cell

differentiation medium. The differentiated cells exhibited immunofluorescence (green) for (E) NGFR, (F) myelin basic protein (MBP), (G) S100 calcium binding protein (S100b), and (H) neural crest marker PAX6. DAPI (blue) is shown in merged images (E-H). The mSKPs were differentiated into (I, J) adipogenic (K) osteogenic cells. The differentiated adipogenic or osteogenic cells from mSKPs were stained by Oil-Red O or Alizarin Red S. Scale bars: 100 μm.

Activation of the Shh pathway by recombinant Shh (rShh) treatment in mSKPs

After treatment of 500 ng/ml rShh, mSKPs in the treated group formed larger spheres than the control group (Fig. 3A, B). Several genes related to stemness, the neural crest, and the Shh pathway was detected in the RT-PCR analysis (Fig. 3C). These findings indicate that sphere formation and multipotency in mSKPs are influenced by activation of the Shh signaling pathway.

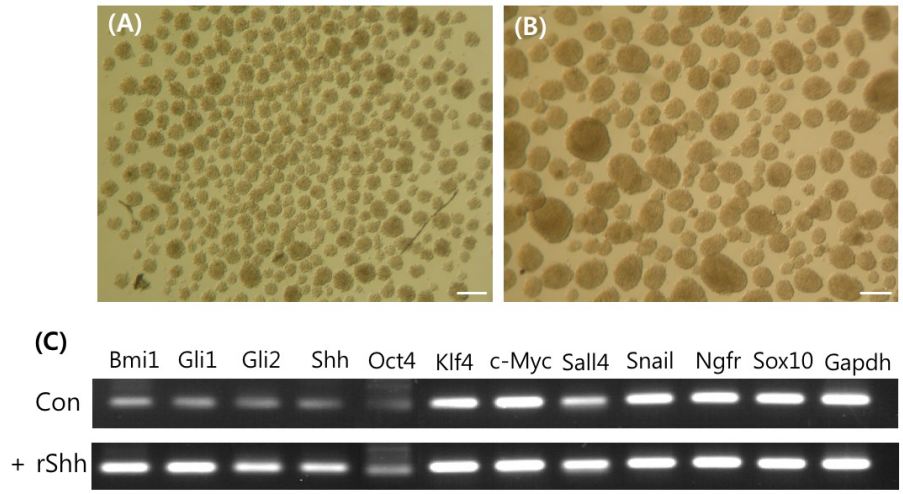

Figure 3. The effect of recombinant Shh (rShh) on mSKPs. The morphology of expanded mSKP spheres; (A) Untreated control. (B) After rShh treatment. (C) RT-PCR analysis of gene expression in mSKPs after rShh treatment. Scale bars: 100 μm.

Treatment with a Shh agonist promotes the proliferation of mSKPs and changes gene expression

The mSKPs treated with Pur (a Shh agonist) formed larger spheres, and their number also increased compared to the control group in all passages checked (Fig. 4A). The results of a WST-1 assay showed a significant increase in the proliferation rate after treatment with Pur at passage 1 and 2 (Fig. 4B). Although the total number of spheres with a diameter over 20 μm was not different from the control group (Fig 4C, panel a), the number of spheres with a diameter over 50 μm increased 5.8-fold and 2.5-fold with Pur treatment at passage 1 and 2, respectively (Fig. 4C, panel b). After Pur treatment, the number of mSKPs at passage 2 was 2-fold higher than at passage 1 (Fig. 4C, panel c). These results show that activation of the Shh signaling pathway by its agonist increases proliferation and sphere formation in mSKPs. A potential critical task of the Shh pathway is the self-renewal of mSKPs.

Treatment with Pur increased the expression of the following genes: c-Myc and Klf4 (reprogramming factors); Ngfr and Nestin (neural progenitor-related markers); CD49f, Sox9, and Bmi1 (stem cell markers); and Smo, Gli1, and Patched1 (Shh pathway-related makers; Fig 5, 6). In addition, Pur treatment increased Gli1 and phosphorylated Akt protein expression. Thus, Pur promotes self-renewal and stemness in mSKPs by increasing the expression of stem cell-,

progenitor-, and reprogramming-related genes via Shh signaling pathway activation.

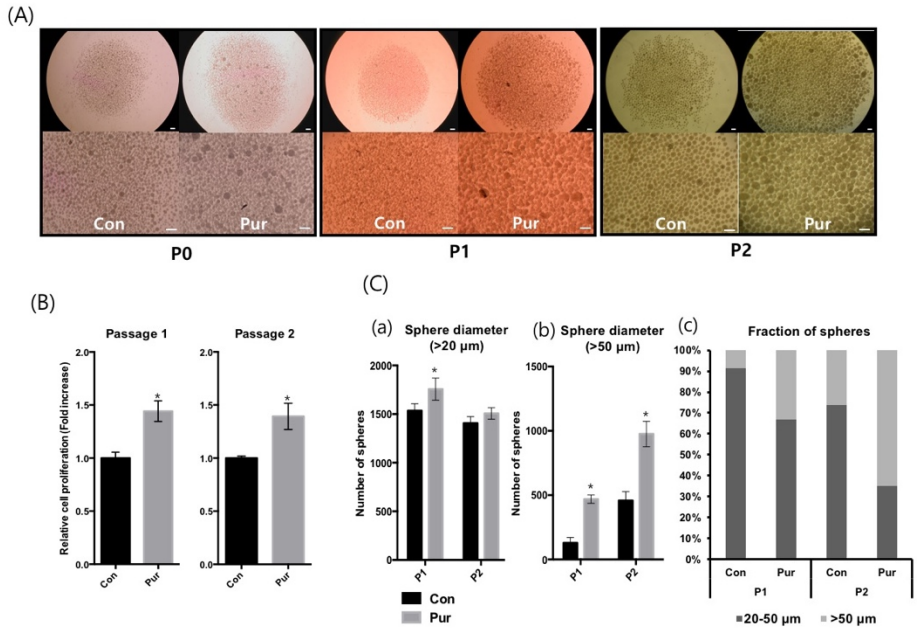

Figure 4. The effect of Purmorphamine (Pur) on mSKPs. (A) mSKP spheres formed at passage 0 (P0), P1, or P2 after Pur treatment. (B) The cell proliferation of mSKPs after Pur treatment was examined by WST-1 assay at P1 and P2. (C) The sphere-forming efficiency of mSKPs was measured. The number of spheres with a diameter more than (a) 20 μm or (b) 50 μm was compared between the control and Pur-treated groups. (c) The relative abundance of large (>50 μm) and small (>20 μm) spheres was measured at P1 and P2. *$p < 0.05$. Scale bars: 100 μm.

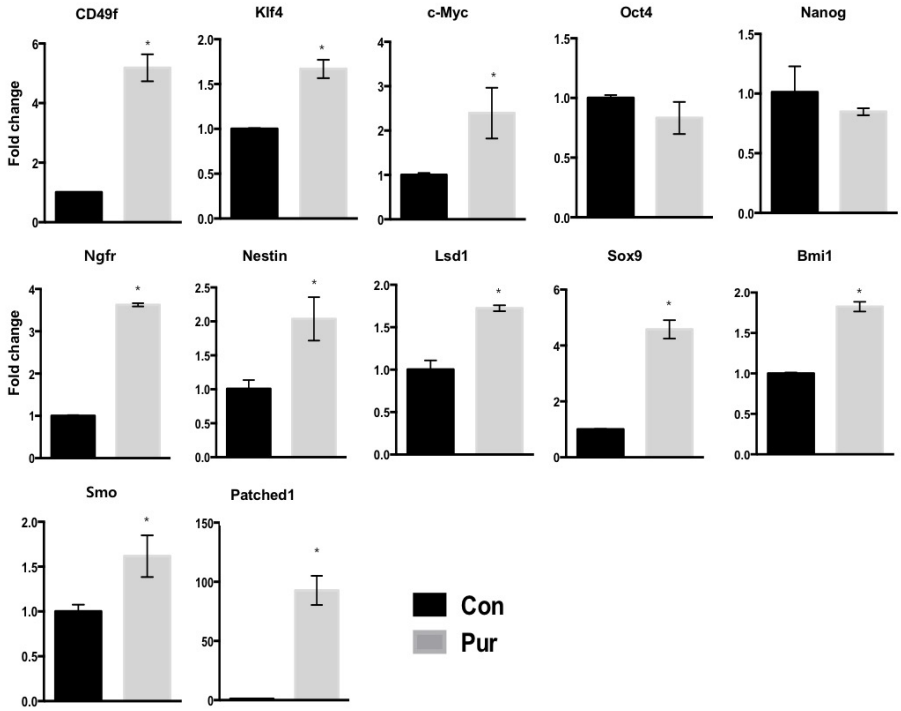

Figure 5. qPCR analyses of mRNA expression in Pur-treated mSKPs. The mRNA expression of Oct4, Nanog, c-Myc, Klf4, N-cad, Twist, Ngfr, Smo, Nestin, Lsd1, Bmi1, Sox9 and Patehed1 was measured by qPCR in mSKPs. Values were normalized against Gapdh and depicted as fold-change values relative to the control (no Pur treatment; control value = 1). *$p < 0.05$.

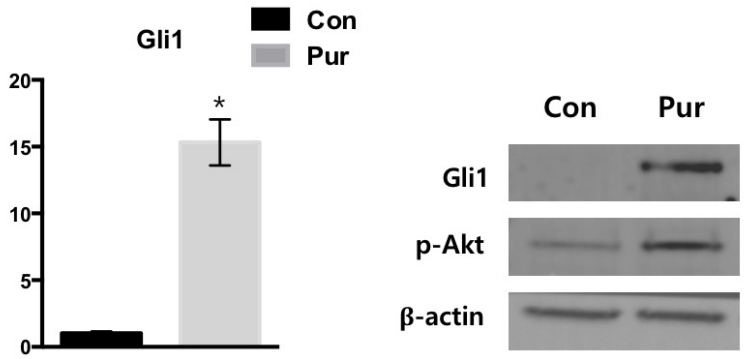

Figure 6. Gli1 expression in Pur-treated mSKPs. The mRNA and protein expression of Gli1 was measured by qPCR or westen blot in mSKPs. Values were normalized against Gapdh and depicted as fold-change values relative to the control (no Pur treatment; control value = 1). *$p < 0.05$.

Treatment with a Smo inhibitor decreases proliferation in mSKPs and changes gene expression

The size and number of spheres decreased after treatment with CP (a shh antagonist), as observed using a stereomicroscope (Fig. 7, 8). A dose-dependent decrease in the proliferation of mSKPs due to CP was also demonstrated by a WST-1 assay (Fig. 9A). Cell morphology and proliferation in CP- and Pur-treated mSKPs were similar to the control group (Fig. 7, 8).
CP treatment decreased the total number of spheres, regardless of their diameter. The number of spheres after co-treatment with CP and Pur was similar to the controls, regardless of diameter. CP-mediated effect was counteracted by Pur treatment (Fig. 9B, panel a-b). In addition, the effect of counteraction by co-treatment showed CP dose-dependent manner on the proliferation and sphere formation of murine SKP (Fig. 9A, B). These results demonstrate that Shh inhibition decreases the formation and proliferation of cellular spheres (Fig. 9B, panel c).

I analyzed mRNA levels of markers in 10 μM CP-treated SKP which most effective treatment on proliferation and sphere formation. Treatment with CP decreased the expression of Gli1 and Smo (Shh pathway genes) and Nestin and Ngfr (neural stem cell/precursor genes). However, the expression of pluripotency and reprogramming genes such as Oct4, Nanog, c-Myc, and Klf4 was not significantly different between the CP-treated and control groups. In

addition, Pur treatment elevated the expression of several key genes which had been decreased by CP treatment (Fig. 10). Therefore, it is possible that Pur treatment may recover a CP-inhibited Shh signaling pathway.

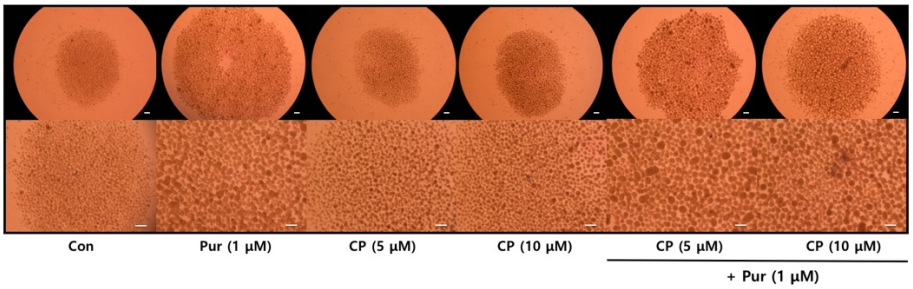

Figure 7. The effect of cyclopamine (CP) on mSKPs at P0. The morphology of mSKPs at P0, after Pur or CP treatment for 72 h. Scale bars: 100 μm

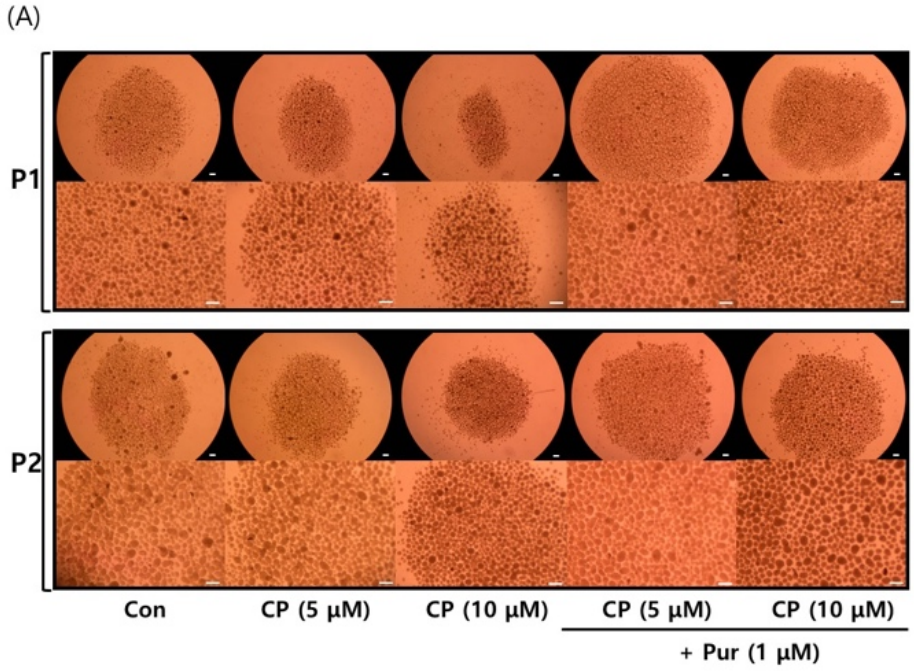

Figure 8. The effect of CP on mSKPs at P1, 2. (A) The mSKP spheres formed in SKP medium at P1 or P2 after combined treatment with CP (5 or 10 μM) and Pur. Scale bars: 100 μm.

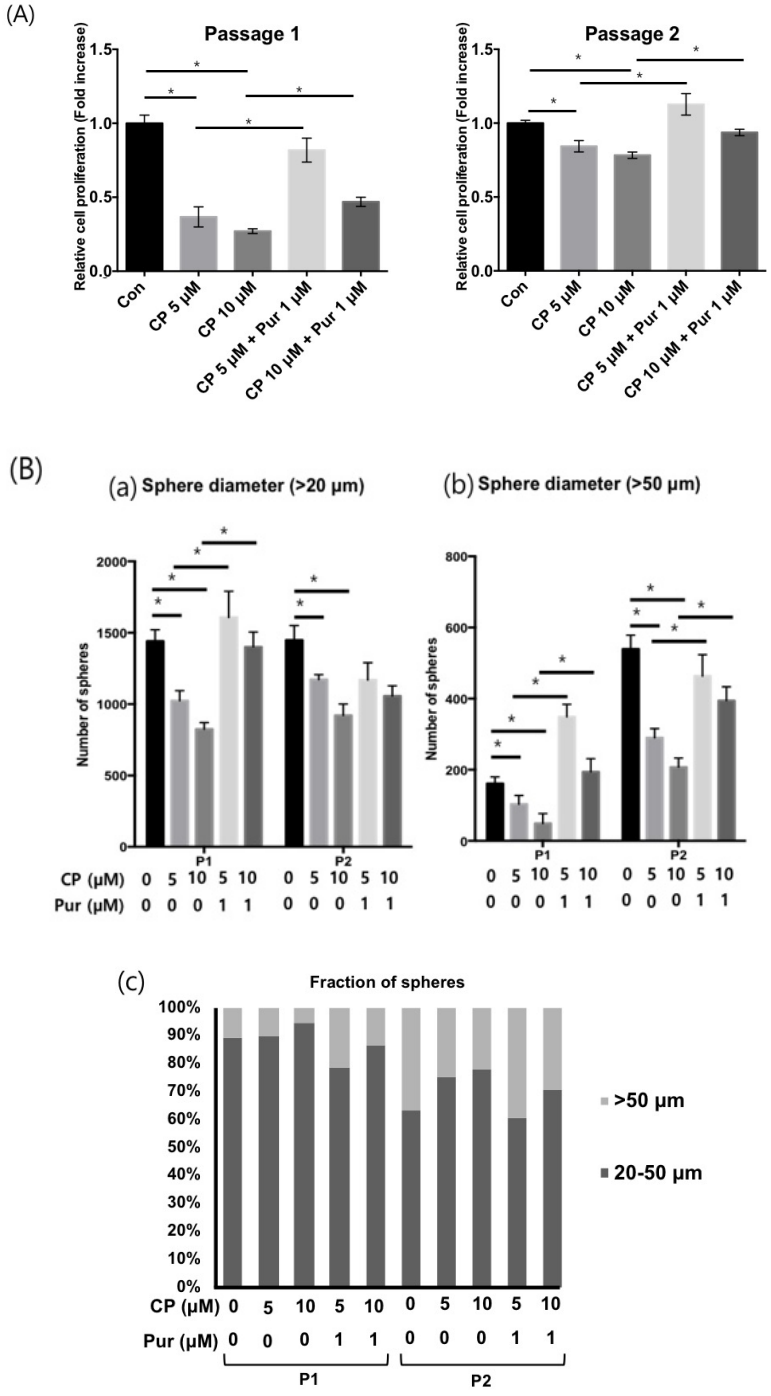
(A)
Passage 1
Passage 2
Relative cell proliferation (Fold increase)
1.5
1.0
0.5
0.0
Con
CP 5 μM
CP 10 μM
CP 5 μM + Pur 1 μM
CP 10 μM + Pur 1 μM
(B)
(a) Sphere diameter (>20 μm)
(b) Sphere diameter (>50 μm)
Number of spheres
2000
1500
1000
500
0
800
600
400
200
P1
P2
CP (μM) 0 5 10 5 10 0 5 10 5 10
Pur (μM) 0 0 0 1 1 0 0 0 1 1
(c)
Fraction of spheres
100%
90%
80%
70%
60%
50%
40%
30%
20%
10%
0%
>50 μm
20-50 μm
CP (μM) 0 5 10 5 10 0 5 10 5 10
Pur (μM) 0 0 0 1 1 0 0 0 1 1
P1
P2

Figure 9. Proliferation analyses of CP-treated mSKPs. (A) Cell proliferation of the mSKPs at P1 and P2 was assessed by WST-1 assay after combined treatment with CP and Pur. (B) The sphere-forming efficiency of mSKPs was measured to confirm the inhibition of Shh signaling pathway by CP and counteraction by Pur in CP-mediated inhibition. The number of spheres with a diameter more than (a) 20 μm or (b) 50 μm was compared between the control, Pur, and CP-treated groups. (c) The relative abundance of large (>50 μm) and small (>20 μm) spheres was measured at P1 and P2 for each treated group. *$p < 0.05$.

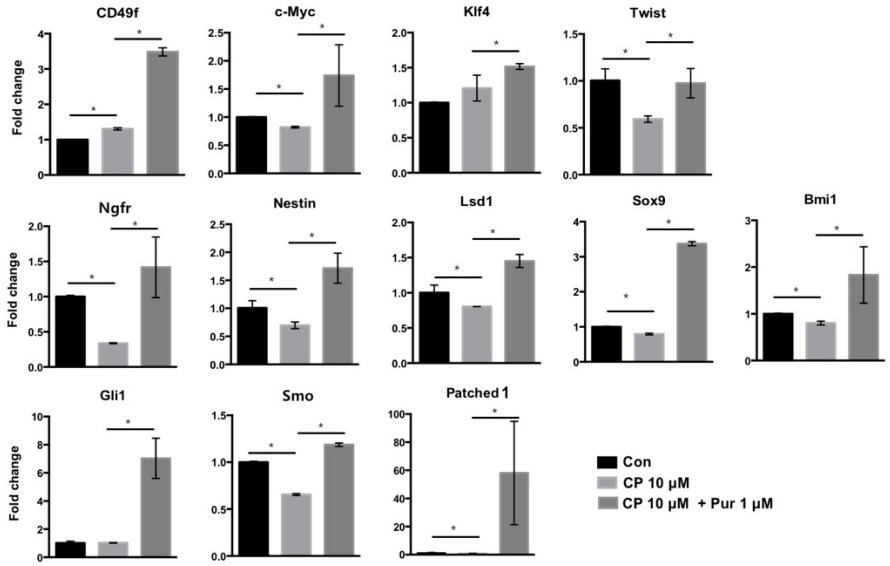

Figure 10. qPCR analyses of mRNA expression in CP-treated mSKPs. The mRNA expression of Oct4, Nanog, c-Myc, Klf4, N-cad, Twist, Ngfr, Smo, Nestin, Lsd1, Bmi1, Sox9, Patehed1, and Gli1 was measured in CP- and Pur-treated mSKPs. Values were normalized against Gapdh and depicted as fold-change values relative to the control (no CP and Pur treatment; control value = 1). *$p < 0.05$.

The effect of a GANT-61 (Gli inhibitor) on the self-renewal and proliferation of mSKPs

The influence of the Shh-Gli signaling pathway on mSKPs was investigated using the Gli inhibitor GANT-61. Treatment of mSKPs with GANT-61 led to reduced sphere formation compared to the control (Fig 11A), and cell proliferation also decreased at passage 2 (Fig. 11B). Sphere size and number were also reduced by Gli1 inhibition (Fig 11C). In addition, the expression of genes related to stemness and Shh signaling was decreased by the Gli1 inhibitor (Fig. 12). These results demonstrated that the formation and proliferation of mSKP spheres are inhibited by a block of the Shh-Gli1 signaling pathway, caused by a Gli1 inhibitor.

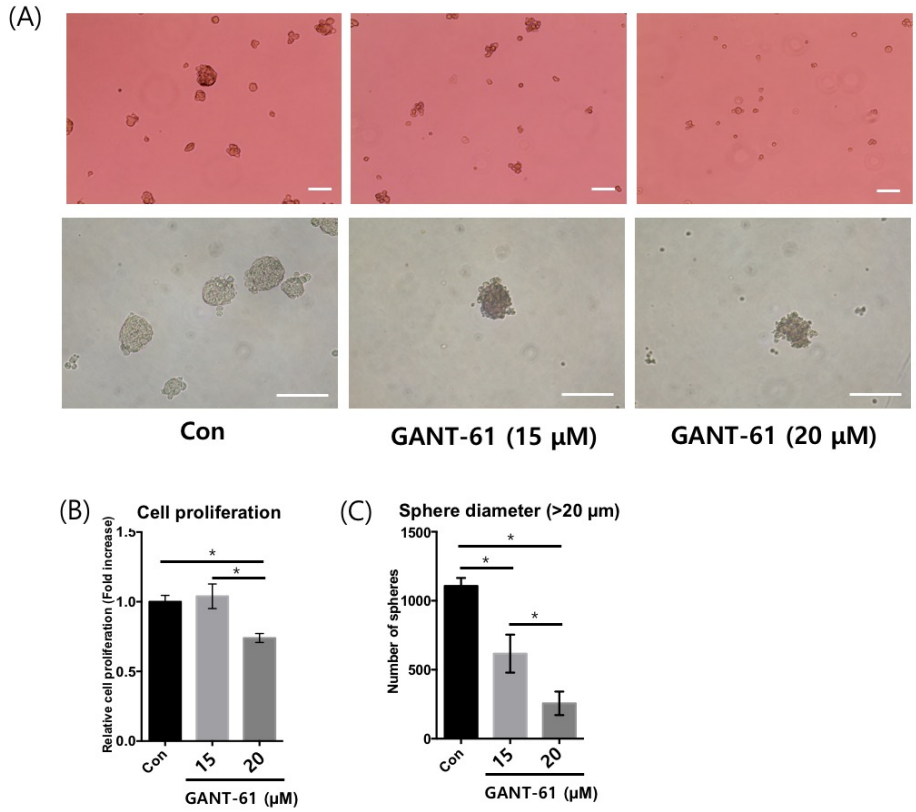

Figure 11. The effect of GANT-61 on mSKPs. (A) The mSKP spheres formed at P2 after GANT-61 (15 or 20 μM) treatment for 72 h. (B) The cell proliferation of mSKPs was examined by WST-1 assay after GANT-61 treatment. (C) The number of spheres with a diameter more than 20 μm was compared between the control and GANT-61 (15 or 20 μM) treatment group. *$p < 0.05$. Scale bars: 100 μm.

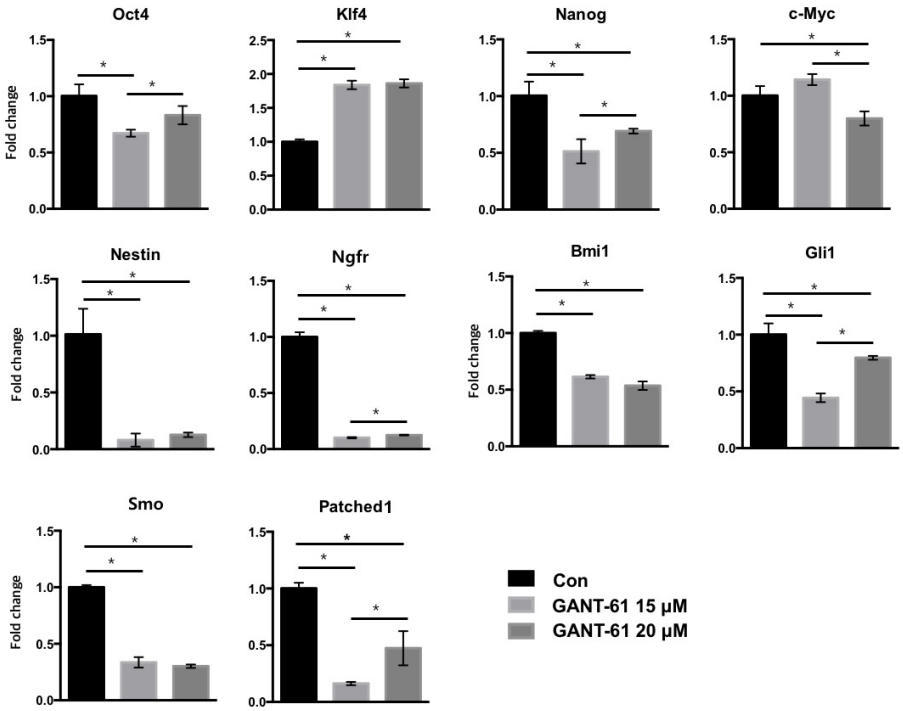

Figure 12. qPCR analyses of mRNA expression in GANT-61-treated mSKPs. The mRNA expression of Nanog, Ngfr, nestin, Bmi1, Patehed1, and Gli1 was measured by qPCR after GANT-61 treatment. Values were normalized against GAPDH and depicted as fold-change values relative to the control (no GANT-61 treatment; control value = 1). *$p < 0.05$

Treatment with CP or GANT-61 influences apoptosis in mSKPs

CP treatment increased apoptosis in mSKPs. In particular, CP induced early apoptosis and resulted in a decrease of live cells. Co-treatment with Pur and CP increased live cells and yielded fewer early apoptotic cells (Fig 13). GANT-61 also decreased live cells and induced both early and late apoptosis. It did this dramatically, in a dose-dependent manner via Gli1 inhibition (Fig. 14). The data demonstrate that Smo or Gli1 inhibition by CP or GANT-61 induces apoptosis and inhibits sphere formation. This result shows that the Shh signaling pathway directly regulates the self-renewal of mSKPs.

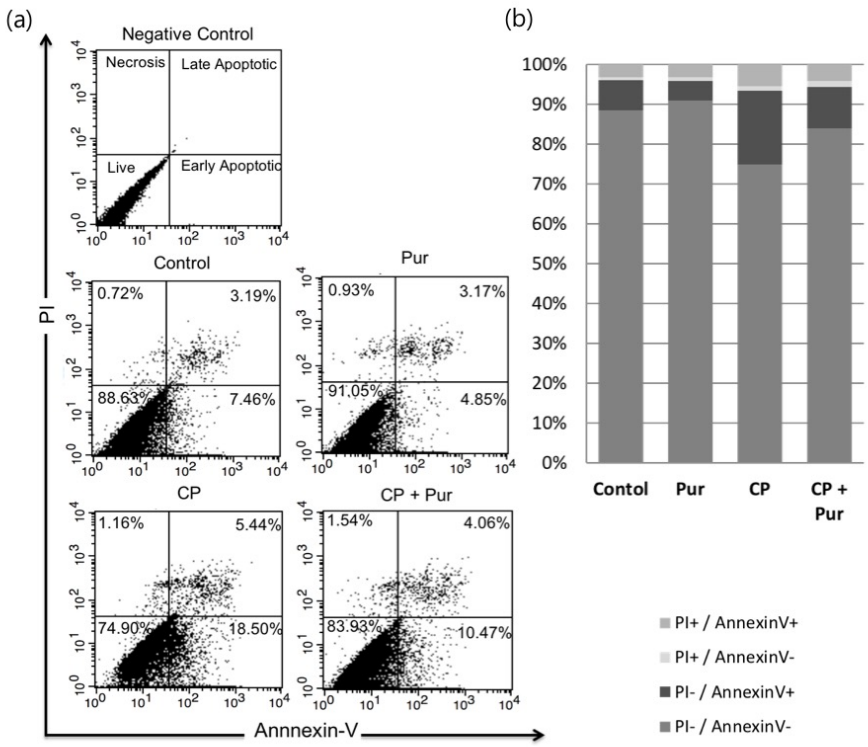

Figure 13. Apoptosis of mSKPs after treatment with CP Apoptotic cells were analyzed by flow cytometry in CP- and Pur-treated mSKPs. Representative biparametric flow cytometry data are derived from combined PI- and FITC-conjugated Annexin V staining. Percentage of PI+/Annexin V- (top left), PI+/Annexin V+ (top right), PI-/Annexin V+ (bottom right), and PI-/Annexin V- (bottom left). (a) Percentage of sorted cells in each quadrant. (b) flow cytometry data represented by a 100% stacked column chart. n = 4.

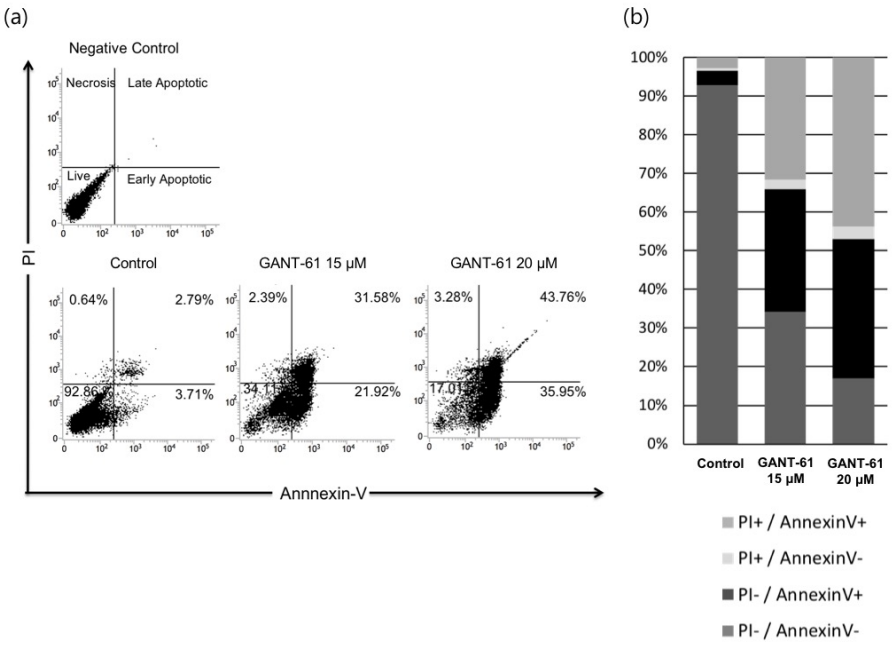

Figure 14. Apoptosis of mSKPs after treatment with GANT-61. Apoptotic cells were analyzed by flow cytometry in GANT-61 (15 or 20 μM)-treated mSKPs. Representative biparametric flow cytometry data are derived from combined PI- and FITC-conjugated Annexin V staining. Percentage of PI+/Annexin V- (top left), PI+/Annexin V+ (top right), PI-/Annexin V+ (bottom right), and PI-/Annexin V- (bottom left). (a) Percentage of sorted cells in each quadrant. (b) flow cytometry data represented by a 100% stacked column chart. n = 4.

The Shh signaling pathway regulates the EMT in mSKPs

To examine the correlation between the Shh signaling pathway and the EMT in mSKPs, expression levels of EMT markers (such as α-Sma, N-cad, Fn1, Vim, and Tgf-β1) were compared between Pur-treated and non-treated mSKPs. The expression of EMT markers was increased by Shh activation, whereas expression was decreased by Shh inhibition. In addition, Pur recovered EMT markers that were inhibited by CP treatment. The Pur-promoted activation of the Shh signaling pathway elevated EMT protein levels, as measured by Western blot and immunofluorescence (Fig. 15). In contrast, inhibition of the Shh signaling pathway by CP decreased EMT protein expression (Fig. 16A). Among the EMT genes, α-Sma and N-cad were strongly affected by the Pur and CP treatments (Fig. 16B). The result shows that the Shh signaling pathway also regulates the EMT phenotype in mSKPs.

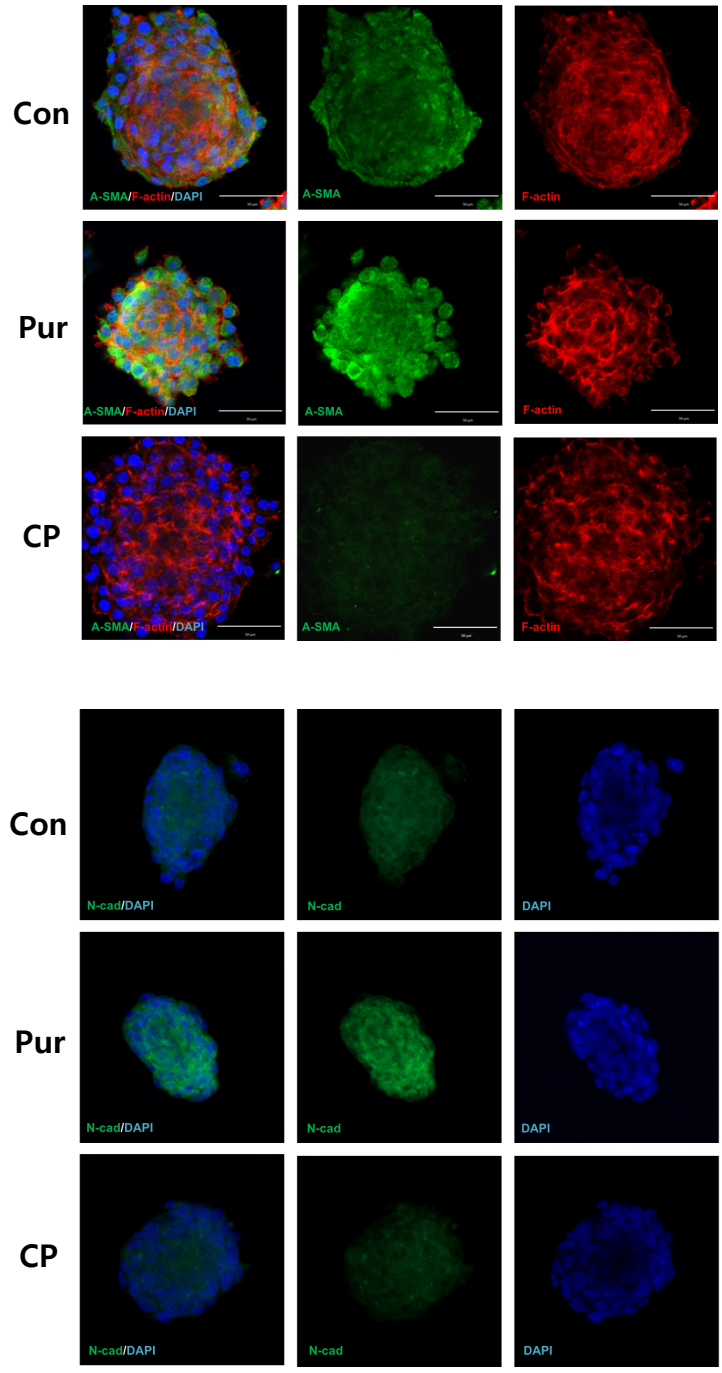
Con
A-SMA/F-actin/DAPI
A-SMA
F-actin
Pur
A-SMA/F-actin/DAPI
A-SMA
F-actin
CP
A-SMA/F-actin/DAPI
A-SMA
F-actin
Con
N-cad/DAPI
N-cad
DAPI
Pur
N-cad/DAPI
N-cad
DAPI
CP
N-cad/DAPI
N-cad
DAPI

Figure 15. Immunostaining of epithelial–mesenchymal transition (EMT) markers by the Shh signaling pathway. The mSKP spheres after CP or Pur treatment were stained with α-Sma or N-cadherin (N-cad; green), and with F-actin (red). DAPI (blue) indicates nuclei. Scale bars: 50 μm.

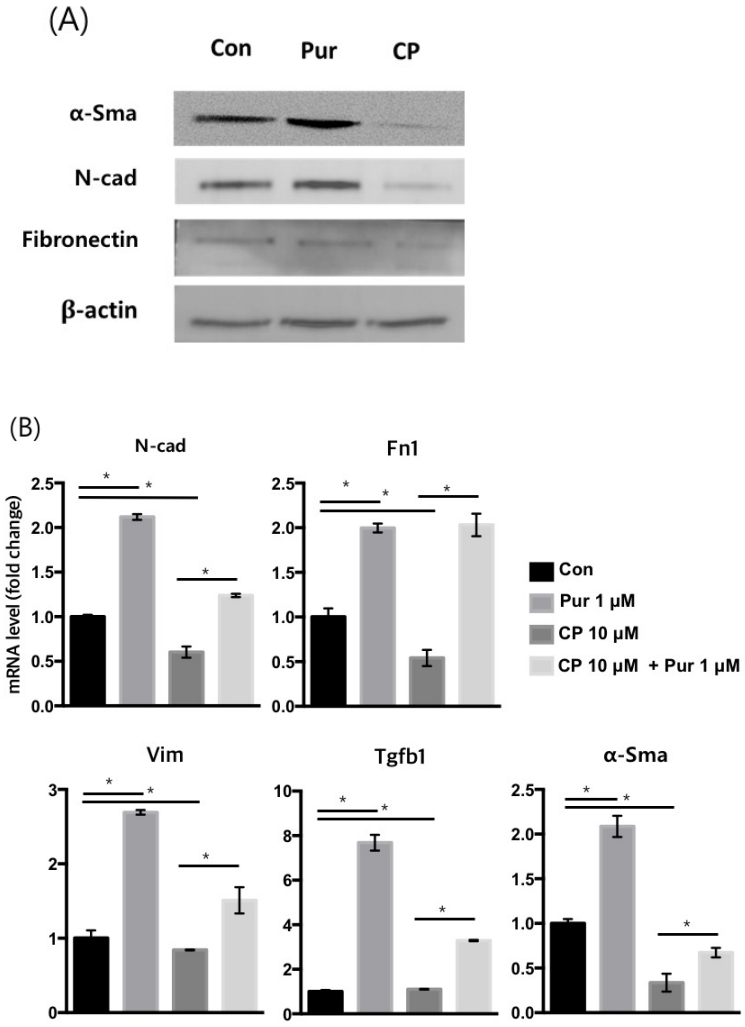

Figure 16. Regulation of EMT genes and protein by the Shh signaling pathway. (A) The relative protein levels of α-Sma, N-cad, and Fibronectin were analyzed by Western blot analysis. The housekeeping protein β-actin was used to control for loading. (B) The mRNA expression of α-Sma, N-cadherin

(N-cad), vimentin (Vim), fibronectin (Fn1), and Tgf-β1 was measured by qPCR in CP-treated mSKPs (with or without Pur) at 72 h. *$p < 0.05$.

Using Pur to promote activation of the Shh signaling pathway for the long-term culture of mSKPs

Although sphere formation in mSKPs was remarkably decreased after passage 3, proliferation and sphere formation in mSKPs were improved by Pur treatment (Fig. 17A, B). These data suggest that activation of the Shh signaling pathway by Pur can revive the self-renewal and proliferation of aged mSKPs.

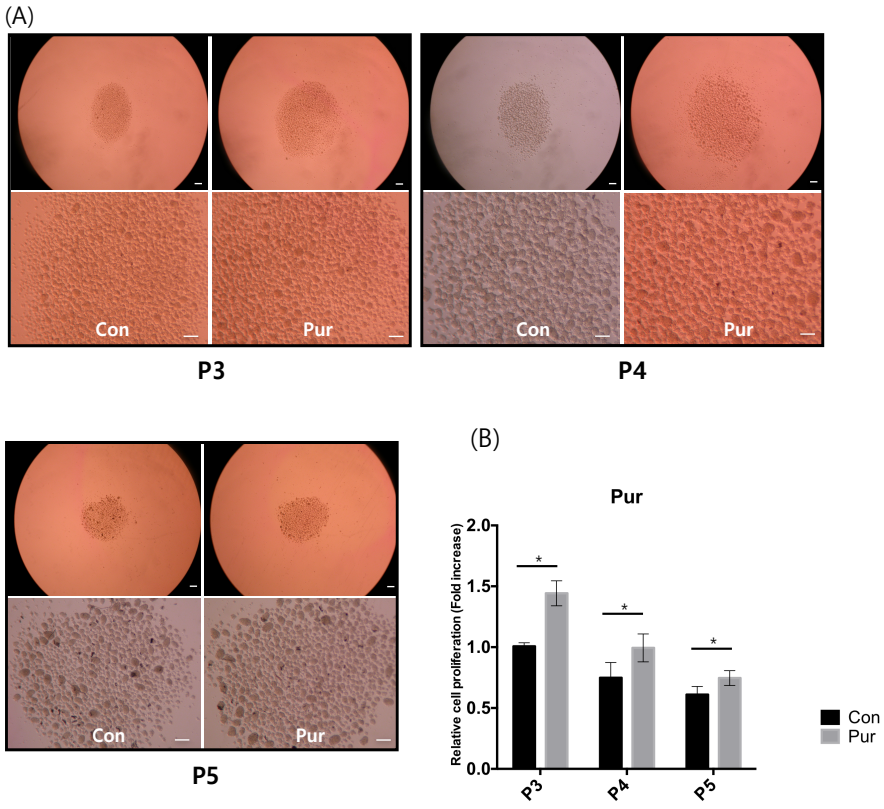

Figure 17. The effect of Pur treatment during long-term culture of mSKPs.

(A) The mSKP spheres formed at P3, P4, and P5 after Pur treatment. (B) The cell proliferation of mSKPs was examined by WST-1 assay after Pur treatment. *$p < 0.05$. Scale bars: 100 μm.

ALP staining after whole SKPs binding on the culture plate

SKPs were seeded and attached on vitronectin-coated dish or tissue culture dish. Attached SKPs with Pur showed two types morphologies as colonized cells (central cells) and migrating cells (marginal cells). However, cultured SKPs in basic SKP medium without Pur did not show colonized cells. These cells were confirmed by ALP staining. Colonized cells were strongly ALP-positive, but migrated cells were negative (Fig. 18A). So, attached SKPs were analyzed by RT-PCR after separation to colonized part and migrated part. The colonized part was increased pluripotency-, reprogramming-related markers than migrated cells or non-treatment group of Pur (Fig. 18B). The level of pluripotent genes expression was confirmed by quantitative real-time PCR. Reprogramming and pluripotency-related markers such as Oct4, Nanog, Sall4 and Rex1 were significantly increased in colonized cells as compared with control group and spread cells. Klf4 and c-Myc were decreased in colonized cells because expression levels of Klf4 and c-Myc in SKPs was originally higher than pluripotent stem cells on the vitronectin-coated dish (Fig. 19). These results indicate the activation of shh signaling by Pur promotes stemness of attached SKPs on vitronectin-coated dish.

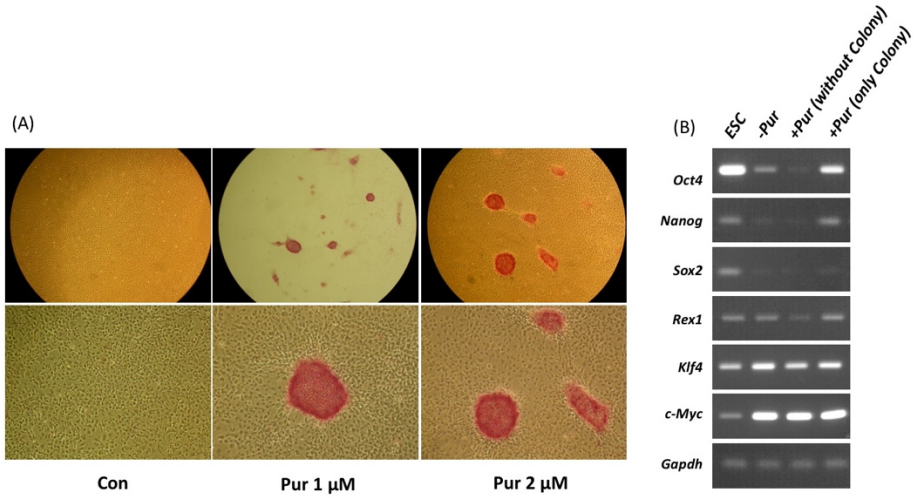

Figure 18. Stemness property of seeded SKPs with Pur. (A) SKPs were seeded on the vitronectin-coated plate and seeded SKPs were cultured on SKP medium with Pur 1 and 2 μM for 7 days. Seeded SKPs were stained by alkaline phosphatase after 7 days. (B) Expression of pluripotency, reprogramming markers including Oct4, Nanog, Sox2, Rex1, Klf4 and c-Myc was analyzed by RT-PCR in seeded SKPs. Positive control is murine embryonic stem cells (ESCs). Scale bars: 100 μm.

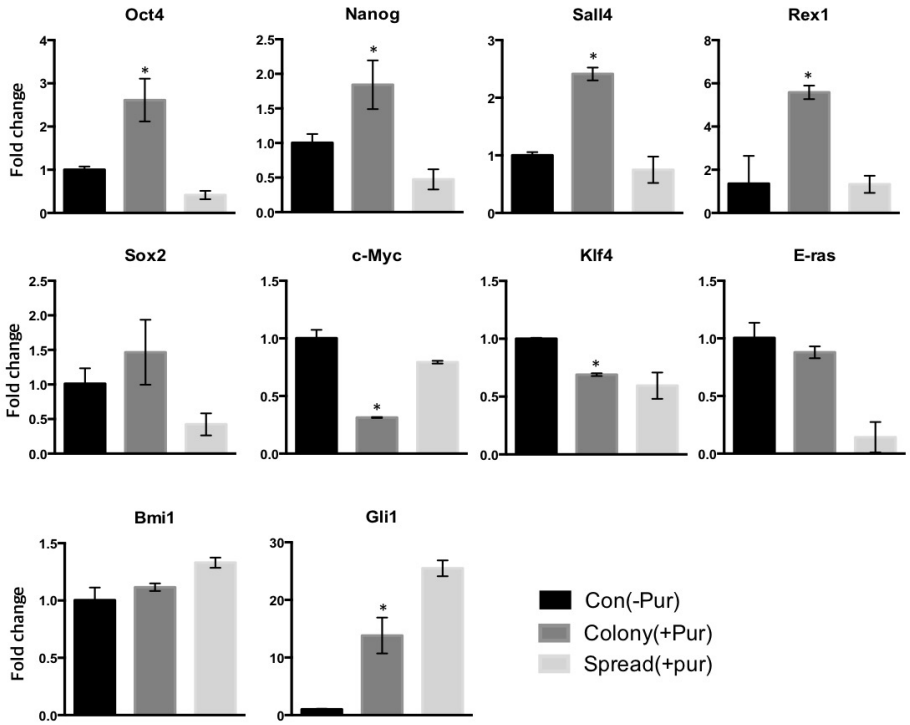

Figure 19. qPCR analyses of mRNA in seeded SKPs treated with Pur. Expression level of the mRNA of Oct4, Nanog, Sall4, Rex1 Sox2, c-Myc, Klf4, E-ras, Bmi1 and Gli1 were measured in seeded SKPs treated with Pur and only SKPs for 7 days. Values were normalized against Gapdh and depicted by the rate to the expression in control group (without chemical treatment; values in non-treated SKPs = 1). $*p < 0.05$.

Treatment with IGF1 promotes the proliferation of mSKPs and changes gene expression

The mSKPs treated with 100 ng/ml IGF1 formed larger spheres, and their number also increased compared to the control group at passage 2 (Fig. 20A). The results of the WST-1 proliferation assay represented a significant increase in the proliferation rate after treatment with 100 ng/ml IGF1 (Fig. 20B). Although the total number of spheres with a diameter over 20 μm was not different from the control group (Fig. 20C, panel a), the number of spheres with a diameter over 50 μm increased 3.1-fold with IGF1 treatment at passage 2 (Fig. 20C, panel b). These results represent that 100 ng/ml IGF1 treatment increases proliferation and sphere formation in mSKPs.

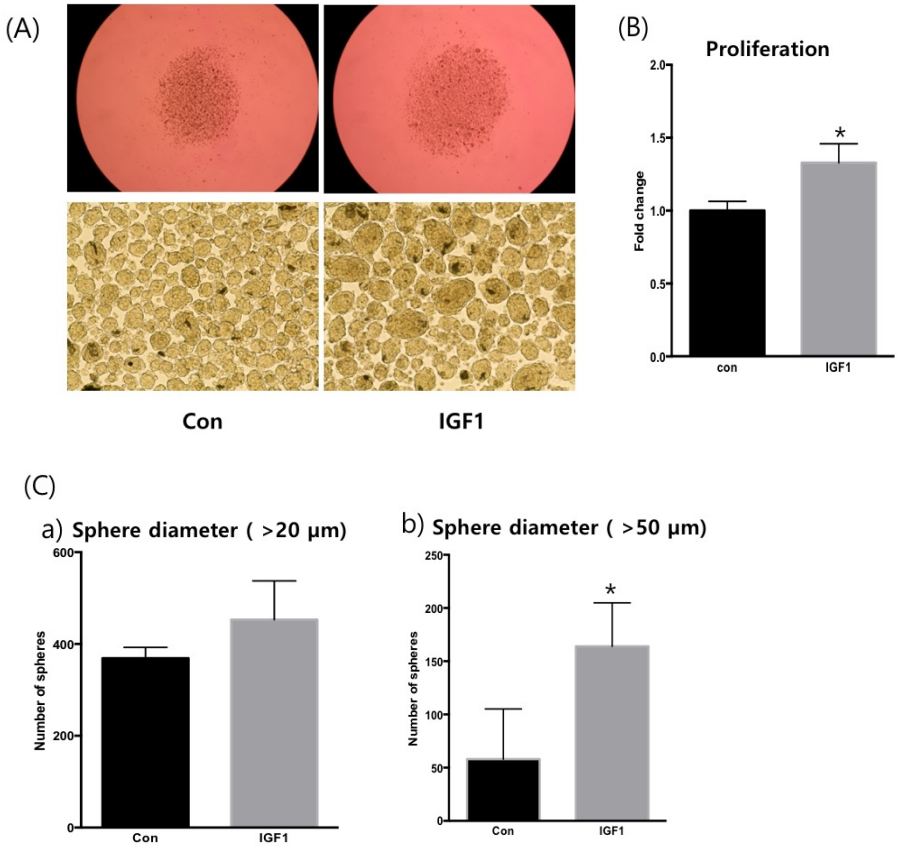

Figure 20. Effect of IGF1 on mSKPs. (A) mSKP spheres formed at passage 2 (P2) after IGF1 treatment. (B) The cell proliferation of mSKPs after IGF1 treatment was examined by WST-1 assay at P2. (C) The sphere-forming efficiency of mSKPs was measured. The number of spheres with a diameter more than (a) 20 μm or (b) 50 μm was compared between the control and IGF1-treated groups. (c) The relative abundance of large (>50 μm) and small (>20 μm) spheres was measured at P2. *$p < 0.05$. Scale bars: 100 μm.

Treatment with IGF1 regulates the EMT phenotype in mSKPs

To investigate the interaction between the IGF1 signaling pathway and the EMT in mSKPs, expression levels of EMT markers (such as N-cad, Fn1, Vim, S100a4, Snai2 and Tgf-β1) were compared between IGF1-treated and non-treated mSKPs. The expression of EMT markers was upregulated by IGF1 treatment. (Fig. 21A). The IGF1 treatment increased EMT markers such as N-cadherin (N-cad) and vimentin (Vim), as analyzed by immunofluorescence (Fig. 21B). The results show that the IGF1 treatment induced the EMT phenotype in mSKPs.

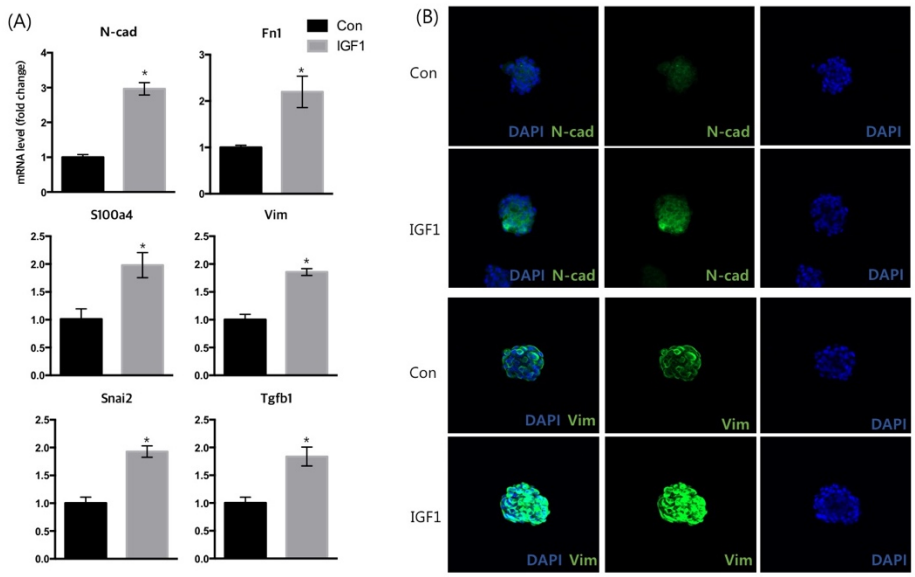

Figure 21. Change of epithelial–mesenchymal transition (EMT) genes by the IGF1. (A) The mRNA expression of N-cadherin (N-cad), vimentin (Vim), fibronectin (Fn1), S100a4, Snai2 and Tgf-β1 was measured by qPCR in IGF1-treated mSKPs at 72 h. Values were normalized against Gapdh and depicted as fold-change values relative to the control (no IGF1 treatment; control value = 1). (B) The mSKPs after IGF1 treatment were stained with Vim (green) or N-cadherin N-cad (green). DAPI (blue) indicates nuclei. *$p < 0.05$. Scale bars: 50 μm.

Treatment with H_2O_2 decreases proliferation in mSKPs

To investigate the damage of H_2O_2 on mSKPs, they were treated to various concentrations of H_2O_2 in the culture medium for 24 h. The size and number of spheres decreased after treatment with H_2O_2 at 200 μM, as observed using a stereomicroscope (Fig. 22A). Treatment of mSKPs with H_2O_2 at 200 or 500 μM significantly decreased cell proliferation compared to the control group (Fig. 22B).

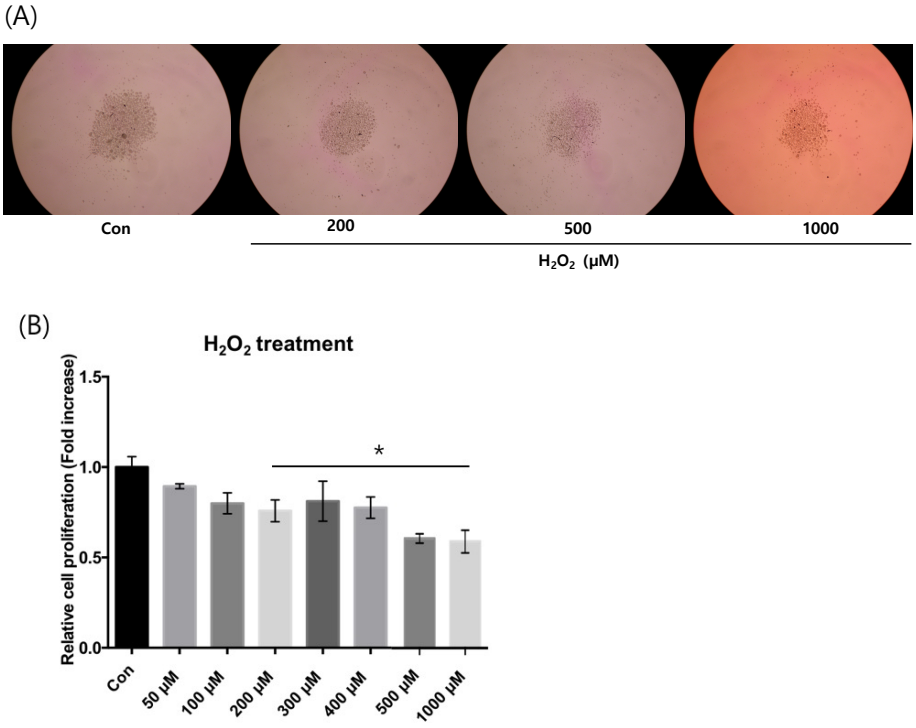

Figure 22. Effect of H_2O_2 on mSKPs. (A) The mSKP spheres formed at P2 after H_2O_2 treatment from 200 to 1000 μM for 72 h (B) The proliferation of mSKPs was analyzed after treating the cells with different concentrations of H_2O_2 from 50 to 1000 μM by WST-1 assay at P2. *$p < 0.05$. Scale bars: 100 μm.

Treatment of IGF1 reduces damage of H_2O_2-induced mSKPs

To evaluate whether IGF1 reduced H_2O_2-induced damage in SKPs, the cell proliferation and morphology of H_2O_2-treated mSKPs were analyzed with IGF1 treatment. H_2O_2-induced damage was significantly attenuated by the treatment of IGF1 (Fig. 23A). In addition, SA-β-gal staining was performed to confirm the progression of senescence. The number of β-gal-positive SKPs increased in H_2O_2 treatment for 48 h. However, Co-treatment with H_2O_2 and IGF1 decreased β-gal-positive SKPs (Fig. 23B). This indicates that the H_2O_2-induced senescent cell population is reduced by IGF1 treatment. Therefore, IGF1 treatment may decrease the damage of SKPs during *in vitro* culture.

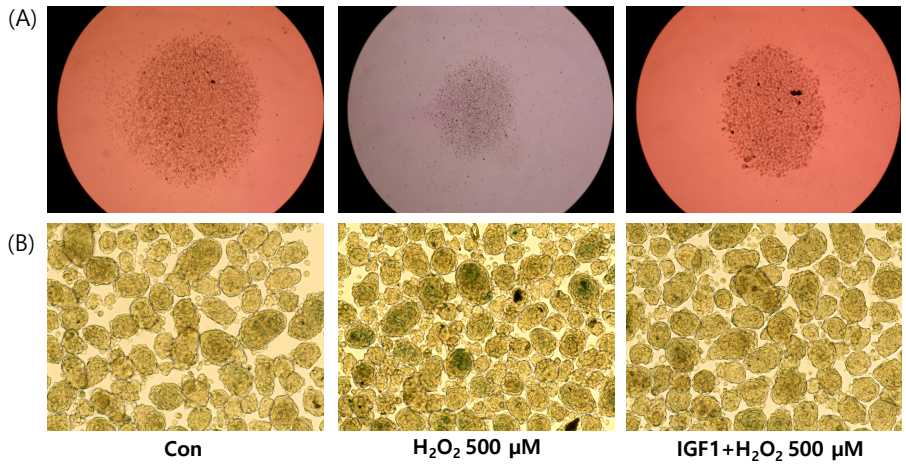

Figure 23. Effect of IGF1 on H_2O_2-treated mSKPs. (A) The mSKP spheres formed in SKP medium at P2 after combined treatment with IGF1 and 500 μM H_2O_2 for 72 h. (B) The SA-β-gal activity analysis performed on the H_2O_2-treated mSKPs with or without IGF1 treatment, and β-gal positive spheres detected. Scale bars: 100 μm.

Treatment of IGF1 reduces the generation of ROS

To examine the effects of IGF1 on the ROS production, intracellular ROS levels of mSKPs were analyzed by DCF-DA assay. The fluorescence intensity level of DCF-DA was significantly higher in the H_2O_2 treatment group than in the non-treatment group for 24 or 72 h. However, co-treatment with H_2O_2 and IGF1 decreased the fluorescence intensity of DCF-DA in SKPs a level similar to the non-treatment group (Fig. 24). This demonstrates that the H_2O_2-induced generation of ROS is reduced by IGF1 treatment.

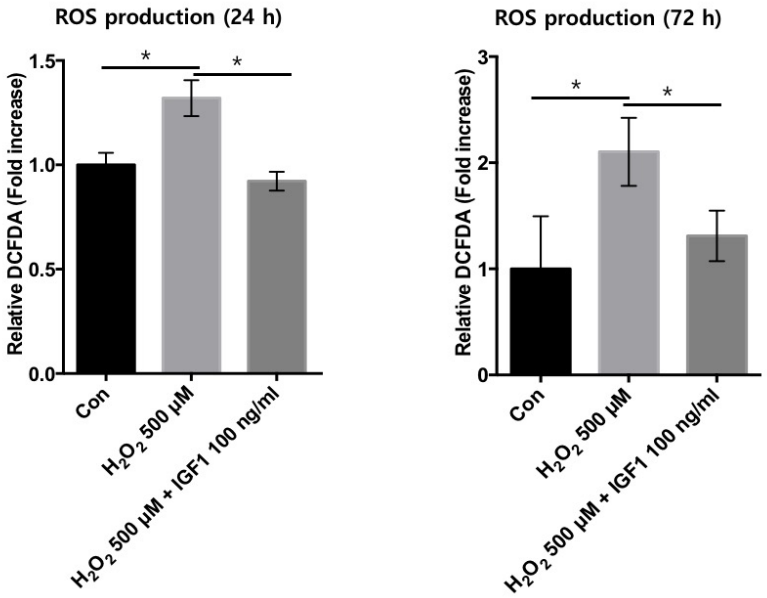

Figure 24. Analysis of ROS levels in mSKPs after treatment with H_2O_2 and IGF1. ROS level was assessed by DCFDA assay after combined treatment with IGF1 and H_2O_2 for 24 or 72 h. Values were depicted as fold-change values relative to the control (no IGF1 and H_2O_2 treatment; control value = 1). *p < 0.05.

Treatment of IGF1 induces the expression of antioxidant regulatory factors

To examine the correlation between IGF1 and the oxidative stress in mSKPs, expression levels of oxidative stress-related markers (such as GPX1, HO-1 and Nrf2) and IGF1R were compared between IGF1-treated and non-treated mSKPs under with H_2O_2 (Fig 25A). The expression of IGF1R was increased by IGF1 treatment with H_2O_2 but decreased when only treated with H_2O_2 . The expression of oxidative stress-related markers also decreased by IGF1 under with H_2O_2 treatment than only H_2O_2 treatment. In addition, the IGF1 treatment elevated levels of antioxidant regulatory protein such as Nrf2 and GPX1, as measured by Western blot (Fig. 25B). Thus, IGF1 also has an effect on the activation of antioxidant-related protein in mSKPs.

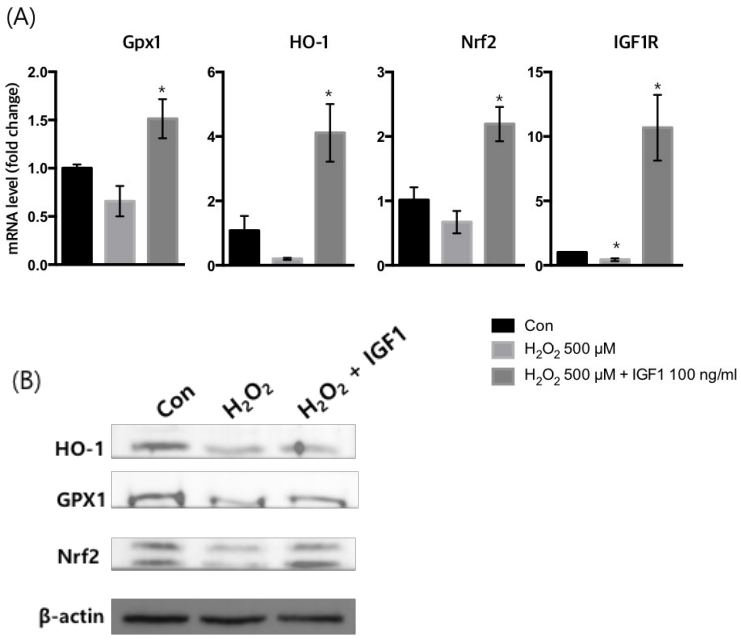

Figure 25. Analyses of anti-oxidative stress makers using qPCR and western blot in H_2O_2-treated mSKPs with IGF1. (A) The mRNA expression of Gpx1, HO-1, Nrf2 and IGF1R was measured in H_2O_2-treated mSKPs (with or without IGF1) for 72 h. Values were depicted as fold-change values relative to the control (no IGF1 and H_2O_2 treatment; control value = 1) (B) The relative protein levels of HO-1, GPX1 and Nrf2 were analyzed by western blot analysis. The housekeeping protein β-actin was used to control for loading. $*p < 0.05$.

DISCUSSION

The objective of this study was to investigate sphere formation and cell proliferation of SKPs by Shh signaling pathway using agonist or antagonist and by IGF1 signaling.

In first topic, I demonstrated that Pur increases the expression of stem cell genes (CD49f, Ngfr, nestin, Klf4, and Bmi1) and EMT genes (N-cad, α-Sma, Fn1, Vim, and Tgf-β1) in mSKPs. The findings suggest that Pur promotes the proliferation of mSKPs in culture, and that the Shh signaling pathway regulates the self-renewal of mSKPs. The Hh signaling pathway is involved in the survival, proliferation, and differentiation of cells in embryonic development (Fernandes-Silva *et al.*, 2017; Infante *et al.*, 2015; Liu *et al.*, 2014). Many other studies have shown that aberrant signaling in this pathway is related to a variety of human cancers. These include basal cell carcinomas, colorectal cancer, ovarian cancer, and small-cell lung cancer (Benvenuto *et al.*, 2016; Bermudez *et al.*, 2013; Ke *et al.*, 2015; Zhang *et al.*, 2016). Activation of the Shh signaling pathway has an essential role in controlling self-renewal and tumor initiation in melanoma (Santini *et al.*, 2012). In addition, the Shh signaling pathway increases the initial generation and self-renewal of neural cells (Lai *et al.*, 2003). To our knowledge, there is no available study as to whether the Shh signaling pathway influences the proliferation, self-renewal,

and apoptosis of mSKPs. It were demonstrated that Pur treatment enhances the sphere formation capability of mSKPs, and this result shows that the Shh signaling pathway is related to the self-renewal and proliferation of mSKPs.

It has been suggested that Hh signaling plays a critical role in regulating the proliferation of various types of stem cells, including mammary, telencephalic, and mesenchymal stem cells (Hong *et al.*, 2013). Pur enhances cell proliferation and reduces apoptosis in human umbilical cord blood-derived MSCs. This is achieved through the RNA-binding protein Msi1, which regulates oncogenes, cell cycle genes, and microRNAs (Hong *et al.*, 2013). Pur were used to activate the Shh signaling pathway because it showed a similar effect to rShh. After Pur treatment, mSKPs were evaluated according to sphere size and number to verify the capacity for sphere formation. It has been reported that the PI3K-Akt signaling pathway promotes self-renewal and inhibits senescence in human SKPs treated with small molecules (Liu *et al.*, 2011). The mSKP were confirmed that the number of spheres with a diameter longer than 50 μm increased at passage 1 and 2 after Pur treatment. The results suggest that Pur treatment activates the Shh signaling pathway to promote cell proliferation and self-renewal in SKPs. Although the expression of key pluripotency genes (Oct4 and Nanog) did not change with Pur treatment, neural and adult stem cell markers (Nestin, CD49f, Klf4, and Ngfr) increased, indicating the stemness-enhancing property of Pur.

Shh regulates the self-renewal of stem cells through canonical and non-canonical hedgehog pathways that are related to the Smo receptor (Wu *et al.*, 2010; Zhang *et al.*, 2015). The chemical regulation of Hh signaling may have biomedical applications, such as the treatment of Hh signaling pathway-related cancers or the differentiation of stem cells (Cochrane *et al.*, 2015; Oliveira *et al.*, 2012; Plaisant *et al.*, 2009). The secreted Hh protein binds to Patched1, which represses the activity of Smo in the Hh signaling pathway. This promotes the expression of Hh target genes by affecting Gli family transcription factors (Ke *et al.*, 2015; Zhang *et al.*, 2015; Zhou *et al.*, 2016). Pur also modulates Smo activity through binding to Patched1 (Cohen *et al.*, 2015). The data show that Pur activates the Shh signaling pathway by increasing the expression of Patched1 and Gli1.

The Shh signaling pathway can be inhibited by various small molecules that target disparate members of the pathway (Stanton *et al.*, 2009). In particular, the Smo antagonist CP acts by binding to Smo. CP treatment reduces the proliferation of hippocampal neural progenitor cells *in vivo* and *in vitro*, and cancer cells *in vitro* (Cohen *et al.*, 2015; Fu *et al*., 2004; Lai *et al*., 2003). In the study, sphere proliferation and the number of spheres were reduced by CP treatment in a dose-dependent manner. This result implies that inhibition of the Shh signaling pathway by a Smo antagonist depresses the self-renewal of mSKPs. However, stemness-related genes such as Klf4, CD49f, and c-Myc did not decrease with the Shh signaling pathway inhibition caused by

CP. Although proliferation and clonogenicity in human mesenchymal stem cells decrease with inhibition of the Hh signaling pathway, this does not influence their differentiation potential (Plaisant *et al.*, 2011). Recent studies have shown that CP induces apoptosis and inhibits the proliferation of cancer cells and cancer stem cells (Cochrane *et al.*, 2015). The results after CP treatment suggest that the Shh signaling pathway is important to the apoptosis of mSKPs. In the present study, the Shh signaling pathway was directly inhibited by GANT-61, a Gli1 inhibitor. Gli1 is an essential gene in the Hh signaling pathway and plays an important role in tumor progression (Benvenuto *et al.*, 2016; Fu *et al.*, 2013). The Shh-Gli signaling pathway is abnormally active in certain cancers, and inhibition of Gli function is important to tumor therapy.

In normal tissues, Gli is primarily active in precursor cells. The direct inhibition of Gli1 dramatically induces apoptosis in cancer stem cells and tumor cells (Fu *et al.*, 2013; Zhou *et al.*, 2016). However, the role of Gli1 in SKPs and stem cells is not clear. GANT-61, which directly inhibits Gli, was used to investigate the effect of Gli1 on proliferation, self-renewal, and apoptosis in mSKPs. The ability of GANT-61 to block the Hh-Gli pathway has been reported in many preclinical and basic studies (Besharat *et al.*, 2018; Zhang *et al.*, 2015). GANT-61 primarily represses self-renewal in cancer cells via inhibition of the Shh signaling p athway (Cochrane *et al.*, 2015; Fu *et al.*, 2013; Santini *et al.*, 2012). The data suggest that GANT-61 causes abnormal spheroid

shape formation *in vitro*. Furthermore, apoptosis increased significantly with GANT-61 treatment. These findings imply that the Shh-Gli pathway is critical to self-renewal in mSKPs, and acts by regulating apoptosis.

Changes in EMT gene expression after activation of the Shh signaling pathway were investigated. The Shh signaling pathway affects the EMT, especially during embryonic development and during metastasis in various cancers (Islam *et al.*, 2016; Ke *et al.*, 2015). Self-renewals in pancreatic cancer stem cells decreased with inhibition of the Shh signaling pathway by sulforaphane (Fu *et al.*, 2013). The results show that certain EMT genes (N-cad, α-Sma, vimentin, fibronectin, and Tgf-β1) increased during sphere formation and propagation when Shh was activated by Pur. This increase in EMT gene expression contributes to the self-renewal and proliferation of SKPs, similar to the case in stem cells (Fu *et al.*, 2013; Islam *et al.*, 2016). EMT gene expression decreased after the Shh signaling pathway was inhibited by CP or GANT-61 treatment. These data suggest that the Shh signaling pathway and the EMT are associated with self-renewal and proliferation during sphere formation in mSKPs.

When human and mouse SKPs are cultured long-term, aging and senescence occur. Sphere formation and cell proliferation are reduced, and these cells cannot maintain their self-renewal potency at late passages (Liu *et al.*, 2011). These results show that activation of the Shh signaling pathway by

Pur treatment improves the self-renewal of mSKPs during long-term culture *in vitro*.

The SKPs were seeded on the vitronectin-coated dish and then attached SKP were treated SKP medium with Pur for identification of effect of Pur in attached SKP. The cells migrated out of the sphere to form a flat monolayer in SKP medium and form of sphere spread and disappeared. However, although cells migrated out of the sphere to flat monolayer, form of sphere remained to multilayer in SKP medium with Pur group. The ALP-positive staining colonies appeared at the maintained sphere's form, however control group and flat monolayer part could not have ALP-positive colony. In addition, stemness-related genes expression in ALP-positve part (central multilayer part) and ALP-negative part (migrated monolayer part) was analyzed by quantitative PCR. Genes expression of ALP-positive part were increased by Pur, but not in ALP-negative part in Pur treatment. The previous study, Shh signaling activation induced Bmi1 expression and increasing Bmi1 and Oct4 transfection could generate iPSCs from fibroblast. These results suggest that Pur increases pluripotency-related genes in mSKPs.

In conclusion, first study suggests that the Shh-Gli signaling pathway plays an important role in the self-renewal, proliferation, and inhibition of apoptosis in mSKPs. Pur is critical for the expansion of mSKPs since it enhances self-renewal and proliferation by activating the Shh signaling pathway (Fig. 26).

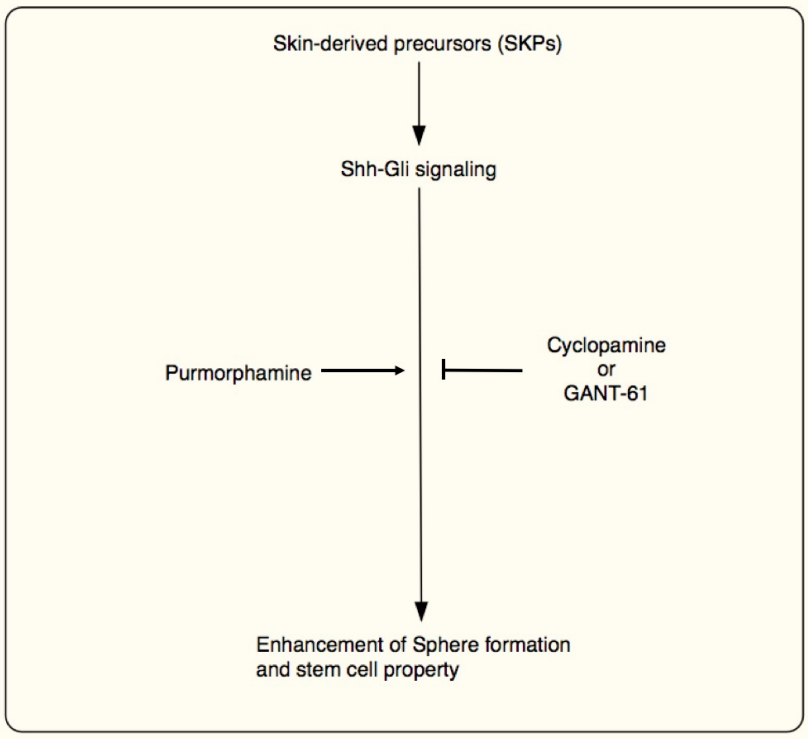

Figure 26. Proposed model for mechanism of shh-Gli signaling pathway by small molecules in mSKPs.

In second study, it was demonstrated that IGF1 increases the expression of EMT markers (N-cadherin, fibronectin, vimentin, S100a4 Snai2 and Tgf-β1) and cell proliferation. It also increases the expression of anti-oxidative stress markers (GPX1, HO-1 and Nrf2) in H_2O_2-treated mSKPs. This findings suggest that IGF1 promotes the proliferation and sphere formation of mSKPs, and decreases the oxidative stress of mSKPs *in vitro* culture.

IGFs play a critical role in stem cell regeneration and longevity (Youssef *et al.*, 2017; Huang *et al.*, 2012; Arsenijevic *et al.*, 2001). IGF1 is especially a crucial factor in the activation and proliferation of neural stem cell. In addition, IGF1 enhances the number and size of the neurosphere, and is essential for continued passaging (Arsenijevic *et al.*, 2001). It has been suggested that IGF1 signaling plays a critical role in regulating the proliferation of various types of stem cells, including neural, dermal, intestine and mesenchymal stem cells (Youssef *et al.*, 2017; Rolfe *et al.*, 2007; Liao *et al.*, 2018; Huang *et al.*, 2012; Arsenijevic *et al.*, 2001). These results were suggested that IGF1 treatment enhances the sphere formation capability of mSKPs, and showed that the IGF1 activation is related to the self-renewal and proliferation of mSKPs.

Changes in the EMT gene expression after treatment of IGF1 were investigated. The IGF1 affects the EMT, especially during stemness maintenance or metastasis in cancer stem cells and various cancers such lung

and Colon. IGF/STAT3/NANOG/Slug signaling axis controls the progression of colorectal cancer by regulation of EMT phenotype and cancer stem cells properties (Yao *et al.*, 2016). This results show that certain EMT genes (N-cad, vimentin, fibronectin, S100a4 and Tgf-β1) increased during sphere formation and propagation by IGF1. This increase in EMT gene expression contributes to the proliferation of SKPs, similar to the case in stem cells.

IGF1 has a significant role in differentiation into neuronal lineage from MSCs by enhancement of proliferation, neurosphere forming, and reduction of apoptosis in the neural progenitor cells (Arsenijevic *et al.*, 2001; Erickson *et al.*, 2008; Tseropoulos *et al.*, 2018). Autocrine IGF1 from human umbilical cord MSCs (hUCMSC) has an effect on cell viability of hUCMSCs via activation of Akt/GSK-3β signaling pathway (Wang *et al.*, 2018). Inhibiting the autocrine IGF1 by blocking IGF1R also reduced hUCMSCs viability and induced apoptosis (Wang *et al.*, 2018). DNA damage can also induce premature senescence. Furthermore, premature cellular senescence can be induced by increased production of ROS (Lu *et al.*, 2008). To evaluate the effects of H_2O_2 on mSKPs, cell proliferation and sphere forming assay were examined. The proliferation of mSKPs treated with 500 μM H_2O_2 was significantly decreased than the control group. Cellular senescence occurs after long culture periods or during the stress of inappropriate growth or physiological environments, and is characterized by telomere uncapping, DNA damage, oxidative stress, and oncogene activity. H_2O_2 induces cellular senescence via generation of ROS in

various cells (Kim *et al.*, 2017; Park, 2013). This result shows that H_2O_2 treatment increases β-gal positive cells and decreases cell proliferation in mSKPs, but these results were recovered by IGF1 treatment. This suggests that IGF1 protects H_2O_2-induced damage in mSKPs.

IGF1 exerted an anti-apoptotic effect by PI3K activation on intestinal epithelial cells in H_2O_2-mediated oxidative stress (Liao *et al.*, 2018). In addition, it guarded retinal pigment epithelial cells by amiodarone-mediated injury via activation of the PI3K/Akt signaling pathway *in vivo* and *in vitro* (Liao *et al.*, 2018). IGF1 is protective effect in a progressive 6-OHDA striatal infusion model (acute animal model of Parkinson's disease) and this protection is performed by activation of pro-survival signaling cascades (Kim *et al.*, 2012). In PC12 cells, IGF1 was also protected against ER stress-induced apoptosis by 6-OHDA. Moreover, IGF1 rescued damaged cells by 6-OHDA via inhibition of ROS production. This data shows that the generation of ROS significantly decreased in the IGF1-treated group compared to the H_2O_2-treated group (Kim *et al.*, 2012). These results suggest that IGF1 treatment influences ROS and oxidative stress pathways. The human dermal stem/progenitor cells-derive conditioned medium (hDSPC-CM) included secreted various growth factors such as bFGF, IGFBP-1, IGFBP-2, HGF, VEGF and IGF1. IGF1 of hDSPC-CM significantly reduced the early and late apoptotic cell population in UVA-irradiated normal dermal fibroblasts (Shim *et al.*, 2013b).

Glutathione peroxidase 1 (GPX1) is a main component of cellular antioxidant and is highly expressed various tissues (Park *et al.*, 2013). IGF1 induces GPX1 expression in human vascular endothelial cells. The oxidative stress and premature senescence of human endothelial cell are reduced by IGF1 treatment. NF-E2-related factor 2 (Nrf2) is a critical factor that regulates expression of endogenous antioxidant enzymes (Zhong *et al.*, 2010). In the present study, mSKP were investigated whether IGF1 was able to regulate the antioxidant mechanism. IGF1 treatment enhanced the expression of anti-oxidative markers such as GPX1 and Nrf2 in gene and protein level on H_2O_2-treated mSKPs. This data suggests that IGF1 treatment protects against H_2O_2-induced oxidative damage by increasing antioxidant regulatory factors (Kim *et al.*, 2012).

In conclusion, second study suggests that the IGF1 plays an important role in the proliferation, and delay of premature senescence against H_2O_2-induced oxidative stress via activation of antioxidant regulatory factor in mSKPs (Fig. 27). The results of this study indicate the IGF1 is able to act antioxidant and oxidative stress research in dermal and neural lineage.

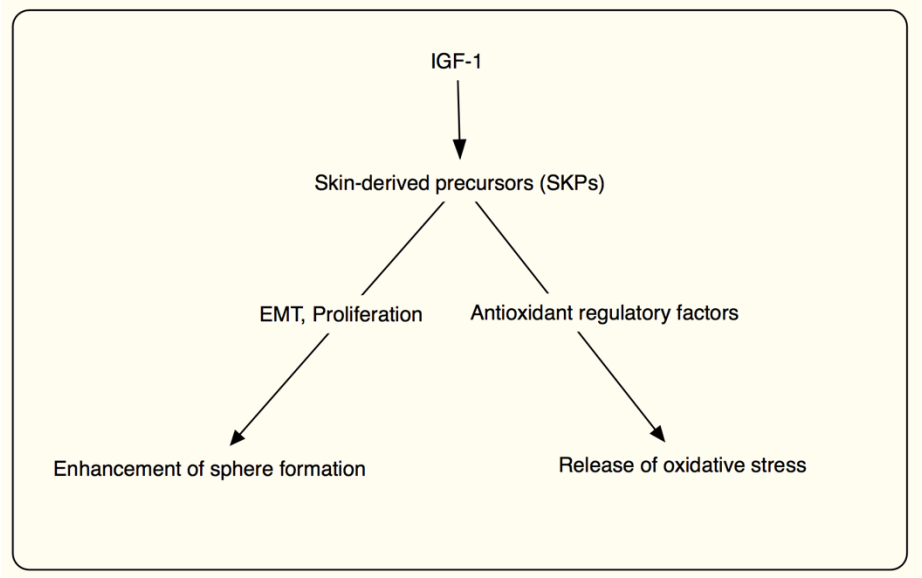

Figure 27. Proposed picture for effect of IGF1 signaling pathway in mSKPs.

CONCLUSION

In the present study, the effects of Shh or IGF1 signaling pathway on the generation and propagation of murine SKPs were investigated using small moleculecus and growth factors (Fig. 31). The Shh-Gli signaling pathway plays a crucial role in the self-renewal, proliferation, and blockade of apoptosis in mSKPs. This study were demonstrated that Pur treatment enhances the sphere formation capability of mSKPs, and this result represents that the Shh signaling pathway is related to the self-renewal and proliferation of mSKPs. Pur is critical for the expansion of mSKPs since it enhances self-renewal and proliferation by activating the Shh signaling pathway. On the other hands, sphere proliferation and the number of spheres were reduced by CP treatment. This result presents that inhibition of the Shh signaling pathway decreases the self-renewal of mSKPs. In addition, GANT-61, Gli antagonist, was used to investigate the effect of Gli1 on proliferation, self-renewal, and apoptosis in mSKPs. This data proposes that GANT-61 causes abnormal spheroid shape formation *in vitro*. These findings imply that the Shh-Gli pathway is critical to self-renewal in mSKPs, and acts by regulating apoptosis. Moreover, Shh signaling pathway and the EMT are associated with self-renewal and proliferation during sphere formation in mSKPs. Shh signaling pathway by Pur treatment improves the self-renewal of mSKPs during long-term culture *in vitro*. The IGF1 acts an

important in the sphere formation, and delay of premature senescence against H_2O_2-induced oxidative stress via activation of antioxidant regulatory factor in mSKPs. IGF1 treatment enhances the sphere formation capability of mSKPs, and IGF1 activation is related to the self-renewal and proliferation of mSKPs. In addition, it protects H_2O_2-induced damage in mSKPs. IGF1 treatment enhanced the expression of anti-oxidative markers such as GPX1 and Nrf2 in gene and protein level on H_2O_2-treated mSKPs. Therefore, IGF1 protects against H_2O_2-induced oxidative damage by increasing antioxidant regulatory factors oxidative damage by increasing antioxidant regulatory factors. The results of this study provided the IGF1 is potentially able to antioxidant for therapeutic use and oxidative stress research in dermal and neural lineage.

However, it remains to be determined these SKPs of different locations has yet to be directly compared, as was assessed for MSCs. The results of these experiments would be of great importance in selection of the source of skin for optimal SKP-based cells therapies. In the future, human SKPs could possibly be grown to sufficient numbers for medical application. The results of this study provide fruitful information that adds to our knowledge of stem cells and skin development and cell proliferation.

Future studies will perform that I can combine reprogramming procedure with various small molecule compounds including Pur and growth factors to activate endogenous expression of reprogramming transcription factors using SKPs. In addition, I will study direct reprogramming into neural

crest stem cell from terminally differentiated cells using small molecules and growth factors.

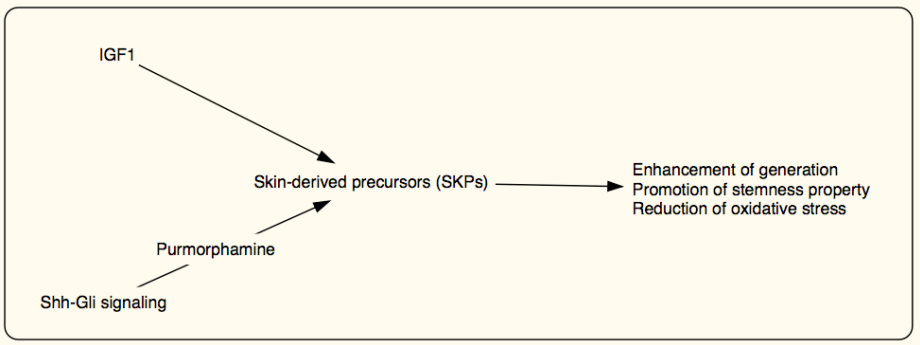

Figure 28. Summary of conclusion. Effect of Shh and IGF1 signaling pathway in skin-derived precursors.

REFERENCE

Alviano F, Fossati V, Marchionni C, Arpinati M, Bonsi L, Franchina M, Lanzoni G, Cantoni S, Cavallini C, Bianchi F, Tazzari PL, Pasquinelli G, Foroni L, Ventura C, Grossi A, Bagnara GP (2007). Term amniotic membrane is a high throughput source for multipotent mesenchymal stem cells with the ability to differentiate into endothelial cells in vitro. BMC Dev Biol **7,** 11.

Arnhold V, Boos J, Lanvers-Kaminsky C (2016). Targeting hedgehog signaling pathway in pediatric tumors: *in vitro* evaluation of SMO and GLI inhibitors. Cancer Chemother Pharmacol **77,** 495-505.

Arsenijevic Y, Weiss S, Schneider B, Aebischer P (2001). Insulin-like growth factor-I is necessary for neural stem cell proliferation and demonstrates distinct actions of epidermal growth factor and fibroblast growth factor-2. J Neurosci **21,** 7194-7202.

Ayadi AE, Zigmond MJ, Smith AD (2016). IGF-1 protects dopamine neurons against oxidative stress: association with changes in phosphokinases. Exp Brain Res **234,** 1863-1873.

Banerjee P, Venkatachalam S, Mamidi MK, Bhonde R, Shankar K, Pal R (2015). Vitiligo patient-derived keratinocytes exhibit characteristics of normal wound healing via epithelial to mesenchymal transition. Exp Dermatol **24,** 391-393.

Baregamian N, Song J, Chung DH (2012). Effects of oxidative stress on intestinal type I insulin-like growth factor receptor expression. Eur J Pediatr Surg **22,** 97-104.

Beattie GM, Lopez AD, Bucay N, Hinton A, Firpo MT, King CC, Hayek A (2005). Activin A maintains pluripotency of human embryonic stem cells in the absence of feeder layers. Stem Cells **23,** 489-495.

Benvenuto M, Masuelli L, De Smaele E, Fantini M, Mattera R, Cucchi D, Bonanno E, Di Stefano E, Frajese GV, Orlandi A, Screpanti I, Gulino A, Modesti A, Bei R (2016). *In vitro* and in vivo inhibition of breast cancer cell growth by targeting the Hedgehog/GLI pathway with SMO (GDC-0449) or GLI (GANT-61) inhibitors. Oncotarget **7,** 9250-9270.

Bermudez O, Hennen E, Koch I, Lindner M, Eickelberg O (2013). Gli1 mediates lung cancer cell proliferation and sonic hedgehog-dependent mesenchymal cell activation. Plos One **8,** e63226.

Besharat ZM, Abballe L, Cicconardi F, Bhutkar A, Grassi L, Le Pera L, Moretti M, Chinappi M, D'Andrea D, Mastronuzzi A, Ianari A, Vacca A, De Smaele E, Locatelli F, Po A, Miele E, Ferretti E (2018). Foxm1 controls a pro-stemness microRNA network in neural stem cells. Sci Rep **8,** 3523.

Biernaskie JA, McKenzie IA, Toma JG, Miller FD (2006). Isolation of skin-derived precursors (SKPs) and differentiation and enrichment of their Schwann cell progeny. Nat Protoc **1,** 2803-2812.

Chambers SM, Fasano CA, Papapetrou EP, Tomishima M, Sadelain M, Studer L (2009). Highly efficient neural conversion of human ES and iPS cells by dual inhibition of SMAD signaling. Nat Biotechnol **27,** 275-280.

Chen T, You YA, Jiang H, Wang ZZ (2017). Epithelial-mesenchymal transition (EMT): A biological process in the development, stem cell differentiation, and tumorigenesis. J Cell Physiol **232,** 3261-3272.

Cochrane CR, Szczepny A, Watkins DN, Cain JE (2015). Hedgehog signaling in the maintenance of cancer stem cells. Cancers (Basel) **7,** 1554-1585.

Cohen M, Kicheva A, Ribeiro A, Blassberg R, Page KM, Barnes CP, Briscoe J (2015). Ptch1 and Gli regulate Shh signalling dynamics via multiple mechanisms. Nat Commun **6**, 6709.

Correa-Costa M, Andrade-Oliveira V, Braga TT, Castoldi A, Aguiar CF, Origassa CST, Rodas ACD, Hiyane MI, Malheiros DMAC, Rios FJO, Jancar S, Camara NOS (2014). Activation of platelet-activating factor receptor exacerbates renal inflammation and promotes fibrosis. Lab Invest **94,** 455-466.

Dai R, Hua W, Xie H, Chen W, Xiong LD, Li L (2018). The human skin-derived precursors for regenerative medicine: current state, challenges, and perspectives. Stem Cells International **2018,** 8637812.

De Bari C, Dell'Accio F, Tylzanowski P, Luyten FP (2001). Multipotent mesenchymal stem cells from adult human synovial membrane. Arthritis Rheum **44,** 1928-1942.

De Kock J, Meuleman P, Raicevic G, Rodrigues RM, Branson S, Meganathan K, De Boe V, Sachinidis A, Leroux-Roels G, Vanhaecke T, Lagneaux L, Rogiers V, Najar M (2014). Human skin-derived precursor cells are poorly immunogenic and modulate the allogeneic immune response. Stem Cells **32,** 2215-2228.

Dupin E, Sommer L (2012). Neural crest progenitors and stem cells: from early development to adulthood. Dev Biol **366,** 83-95.

Dyce PW, Zhu, H., Craig, J. and Li, J. (2004). Stem cells with multilineage potential derived from porcine skin. Biochem Biophys Res Commun 316, 651-8.

Erices A, Conget P, Minguell JJ (2000). Mesenchymal progenitor cells in human umbilical cord blood. Br J Haematol **109,** 235-242.

Erickson RI, Paucar AA, Jackson RL, Visnyei K, Kornblum H (2008). Roles of insulin and transferrin in neural progenitor survival and proliferation. J Neurosci Res **86,** 1884-1894.

Fernandes KJ, McKenzie IA, Mill P, Smith KM, Akhavan M, Barnabé-Heider F, Biernaskie J, Junek A, Kobayashi NR, Toma JG, Kaplan DR, Labosky PA, Rafuse V, Hui CC, Miller FD (2004). A dermal niche for multipotent adult skin-derived precursor cells. Nat Cell Biol **6,** 1082-1093.

Fernandes KJ, Miller FD (2009). Isolation, expansion, and differentiation of mouse skin-derived precursors. Methods Mol Biol **482,** 159-170.

Fernandes KJ, Toma JG, Miller FD (2008). Multipotent skin-derived precursors: adult neural crest-related precursors with therapeutic potential. Philos Trans R Soc Lond B Biol Sci **363,** 185-198.

Fernandes-Silva H, Correia-Pinto J, Moura RS (2017). Canonical sonic hedgehog signaling in early lung development. J Dev Biol **5**, 3.

Forni MF, Ramos Maia Lobba A, Pereira Ferreira AH, Sogayar MC (2015). Simultaneous isolation of three different stem cell populations from murine skin. PLoS One **10,** e0140143.

Fu J, Rodova M, Roy SK, Sharma J, Singh KP, Srivastava RK, Shankar S (2013). GANT-61 inhibits pancreatic cancer stem cell growth *in vitro* and in NOD/SCID/IL2R gamma null mice xenograft. Cancer Lett **330,** 22-32.

Fu M, Lui VCH, Sham MH, Pachnis V, Tam PKH (2004). Sonic hedgehog regulates the proliferation, differentiation, and migration of enteric neural crest cells in gut. J Cell Biol **166,** 673-684.

Garcia-Fernandez M, Castilla-Cortazar I, Diaz-Sanchez M, Navarro I, Puche JE, Castilla A, Casares AD, Clavijo E, Gonzalez-Baron S (2005). Antioxidant effects of insulin-like growth factor-I (IGF-I) in rats with advanced liver cirrhosis. BMC Gastroenterol **5,** 7.

Gingras M, Champigny MF, Berthod F (2007). Differentiation of human adult skin- derived neuronal precursors into mature neurons. J Cell Physiol **210,** 498-506.

Grande MT, Sanchez-Laorden B, Lopez-Blau C, De Frutos CA, Boutet A, Arevalo M, Rowe RG, Weiss SJ, Lopez-Novoa JM, Nieto MA (2015). Snail1-induced partial epithelial-to-mesenchymal transition drives renal fibrosis in mice and can be targeted to reverse established disease. Nature Medicine **21,** 989-997.

Greber B, Lehrach H, Adjaye J (2007). Fibroblast growth factor 2 modulates transforming growth factor beta signaling in mouse embryonic fibroblasts and human ESCs (hESCs) to support hESC self-renewal. Stem Cells **25,** 455-464.

Gros J, Tabin CJ (2014). Vertebrate limb bud formation is initiated by localized epithelial-to-mesenchymal transition. Science **343,** 1253-1256.

Hagner A, Biernaskie J (2013). Isolation and differentiation of hair follicle-derived dermal precursors. Methods Mol Biol **989,** 247-263.

Higashi Y, Sukhanov S, Anwar A, Shai SY, Delafontaine P (2010). IGF-1, oxidative stress and atheroprotection. Trends Endocrinol Metab **21,** 245-254.

Hong IS, Kang KS (2013). The effects of Hedgehog on the RNA-binding protein Msi1 in the proliferation and apoptosis of mesenchymal stem cells. PLoS One **8,** e56496.

Hoogduijn MJ, Gorjup E, Genever PG (2006). Comparative characterization of hair follicle dermal stem cells and bone marrow mesenchymal stem cells. Stem Cells Dev **15**, 49-60.

Huang YL, Qiu RF, Mai WY, Kuang J, Cai XY, Dong YG, Hu YZ, Song YB, Cai AP, Jiang ZG (2012). Effects of insulin-like growth factor-1 on the properties of mesenchymal stem cells *in vitro*. J Zhejiang Univ Sci B **13,** 20-28.

Huangfu DW, Maehr R, Guo WJ, Eijkelenboom A, Snitow M, Chen AE, Melton DA (2008a). Induction of pluripotent stem cells by defined factors is greatly improved by small-molecule compounds. Nat Biotechnol **26,** 795-797.

Huangfu DW, Osafune K, Maehr R, Guo W, Eijkelenboom A, Chen S, Muhlestein W, Melton DA (2008b). Induction of pluripotent stem cells from primary human fibroblasts with only Oct4 and Sox2. Nat Biotechnol **26,** 1269-1275.

Huat TJ, Khan AA, Pati S, Mustafa Z, Abdullah JM, Jaafar H (2014). IGF-1 enhances cell proliferation and survival during early differentiation of mesenchymal stem cells to neural progenitor-like cells. BMC Neurosci **15,** 91.

Hunt DPJ, Jahoda C, Chandran S (2009). Multipotent skin-derived precursors: from biology to clinical translation. Curr Opin Biotech **20,** 522-530.

Hunt DPJ, Morris PN, Sterling J, Anderson JA, Joannides A, Jahoda C, Compston A, Chandran S (2008). A highly enriched niche of precursor cells with neuronal and glial potential within the hair follicle dermal papilla of adult skin. Stem Cells **26,** 163-172.

Infante P, Alfonsi R, Botta B, Mori M, Di Marcotullio L (2015). Targeting GLI factors to inhibit the Hedgehog pathway. Trends Pharmacol Sci **36,** 547-558.

Islam SS, Mokhtari RB, Noman AS, Uddin M, Rahman MZ, Azadi MA, Zlotta A, van der Kwast T, Yeger H, Farhat WA (2016). Sonic hedgehog (Shh) signaling promotes tumorigenicity and stemness via activation of epithelial-to-mesenchymal transition (EMT) in bladder cancer. Mol Carcinogen **55,** 537-551.

Kang PJ, Moon JH, Yoon BS, Hyeon S, Jun EK, Park G, Yun W, Park J, Park M, Kim A, Whang KY, Koh GY, Oh S, You S (2014). Reprogramming of mouse somatic cells into pluripotent stem-like cells using a combination of small molecules. Biomaterials **35,** 7336-7345.

Ke Z, Caiping S, Qing Z, Xiaojing W (2015). Sonic hedgehog-Gli1 signals promote epithelial-mesenchymal transition in ovarian cancer by mediating PI3K/AKT pathway. Med Oncol **32,** 368.

Kim D, Kim H, Kim K, Roh S (2017). The protective effect of indole-3-acetic acid (IAA) on H_2O_2-damaged human dental pulp stem cells is mediated by the AKT pathway and involves increased expression of the transcription factor nuclear factor-erythroid 2-related factor 2 (Nrf2) and its downstream target heme oxygenase 1 (HO-1). Oxid Med Cell Longev **2017,** 8639485.

Kim Y, Li E, Park S (2012). Insulin-like growth factor-1 inhibits 6-hydroxydopamine-mediated endoplasmic reticulum stress-induced apoptosis via regulation of heme oxygenase-1 and Nrf2 expression in PC12 cells. Int J Neurosci **122,** 641-649.

Lai K, Kaspar BK, Gage FH, Schaffer DV (2003). Sonic hedgehog regulates adult neural progenitor proliferation *in vitro* and in vivo. Nat Neurosci **6,** 21-27.

Lebonvallet N, Boulais N, Le Gall C, Cheret J, Pereira U, Mignen O, Bardey V, Jeanmaire C, Danoux L, Pauly G, Misery L (2012). Characterization of neurons from adult human skin-derived precursors in serum-free medium : a PCR array and immunocytological analysis. Exp Dermatol **21,** 195-200.

Levenstein ME, Ludwig TE, Xu RH, Llanas RA, VanDenHeuvel-Kramer K, Manning D, Thomson JA (2006). Basic fibroblast growth factor support of human embryonic stem cell self-renewal. Stem Cells **24,** 568-574.

Li WL, Wei W, Zhu SY, Zhu JL, Shi Y, Lin TX, Hao EG, Hayek A, Deng HK, Ding S (2009). Generation of rat and human induced pluripotent stem cells by combining genetic reprogramming and chemical inhibitors. Cell Stem Cell **4,** 16-19.

Li XJ, Hu BY, Jones SA, Zhang YS, Lavaute T, Du ZW, Zhang SC (2008). Directed differentiation of ventral spinal progenitors and motor neurons from human embryonic stem cells by small molecules. Stem Cells **26,** 886-893.

Liao R, Yan F, Zeng Z, Wang H, Qiu K, Xu J, Zheng W (2018). Insulin-like growth factor-1 activates PI3K/Akt signalling to protect human retinal pigment epithelial cells from amiodarone-induced oxidative injury. Br J Pharmacol **175,** 125-139.

Liu S, Liu S, Wang X, Zhou J, Cao Y, Wang F, Duan E (2011). The PI3K-Akt pathway inhibits senescence and promotes self-renewal of human skin-derived precursors *in vitro*. Aging Cell **10,** 661-674.

Liu Y, Wei ZY, Huang YF, Bai CL, Zan LS, Li GP (2014). Cyclopamine did not affect mouse oocyte maturation *in vitro* but decreased early embryonic development. Anim Sci J **85,** 840-847.

Lu T, Finkel T (2008). Free radicals and senescence. Experimental Cell Research **314,** 1918-1922.

Mahmood A, Harkness L, Schroder HD, Abdallah BM, Kassem M (2010). Enhanced differentiation of human embryonic stem cells to mesenchymal progenitors by inhibition of TGF-beta/Activin/Nodal signaling using SB-431542. J Bone Miner Res **25,** 1216-1233.

Mao D, Yao X, Feng G, Yang X, Mao L, Wang X, Ke T, Che Y, Kong D (2015). Skin-derived precursor cells promote angiogenesis and stimulate proliferation of endogenous neural stem cells after cerebral infarction. Biomed Res Int **2015,** 945846.

McKenzie, IA, Biernaskie J, Toma JG, Midha R, Miller FD (2006). Skin-derived precursors generate myelinating Schwann cells for the injured and dysmyelinated nervous system. J Neurosci **26,** 6651-6660.

Memmi EM, Sanarico AG, Giacobbe A, Peschiaroli A, Frezza V, Cicalese A, Pisati F, Tosoni D, Zhou HQ, Tonon G, Antonov A, Melino G, Pelicci PG, Bernassola F (2015). p63 sustains self-renewal of mammary cancer stem cells

through regulation of Sonic Hedgehog signaling. P Natl Acad Sci USA **112,** 3499-3504.

Moon JH, Yoon BS, Kim B, Park G, Jung HY, Maeng I, Jun EK, Yoo SJ, Kim A, Oh S, Whang KY, Kim H, Kim DW, Kim KD, You S (2008). Induction of neural stem cell-like cells (NSCLCs) from mouse astrocytes by Bmi1. Biochem Bioph Res Co **371,** 267-272.

Naska S, Yuzwa SA, Johnston APW, Paul S, Smith KM, Paris M, Sefton MV, Datti A, Miller FD, Kaplan DR (2016). Identification of drugs that regulate dermal stem cells and enhance skin repair. Stem Cell Reports **6,** 74-84.

Niwa H, Burdon T, Chambers I, Smith A (1998). Self-renewal of pluripotent embryonic stem cells is mediated via activation of STAT3. Gene Dev **12,** 2048-2060.

Oliveira FS, Bellesini LS, Defino HL, da Silva Herrero CF, Beloti MM, Rosa AL (2012). Hedgehog signaling and osteoblast gene expression are regulated by purmorphamine in human mesenchymal stem cells. J Cell Biochem **113,** 204-208.

Osakada F, Jin ZB, Hirami Y, Ikeda H, Danjyo T, Watanabe K, Sasai Y, Takahashi M (2009). In vitro differentiation of retinal cells from human pluripotent stem cells by small-molecule induction. J Cell Sci **122,** 3169-3179.

Park S, Kim H, Kim K, Roh S (2018). Sonic hedgehog signalling regulates the self-renewal and proliferation of skin-derived precursor cells in mice. Cell Prolif **51,** e12500.

Park WH (2013). The effects of exogenous H_2O_2 on cell death, reactive oxygen species and glutathione levels in calf pulmonary artery and human umbilical vein endothelial cells. Int J Mol Med **31,** 471-476.

Plaisant M, Fontaine C, Cousin W, Rochet N, Dani C, Peraldi P (2009). Activation of hedgehog signaling inhibits osteoblast differentiation of human mesenchymal stem cells. Stem Cells **27,** 703-713.

Plaisant M, Giorgetti-Peraldi S, Gabrielson M, Loubat A, Dani C, Peraldi P (2011). Inhibition of hedgehog signaling decreases proliferation and clonogenicity of human mesenchymal stem cells. PLoS One **6,** e16798.

Polisetty N, Fatima A, Madhira SL, Sangwan VS, Vemuganti GK (2008). Mesenchymal cells from limbal stroma of human eye. Mol Vis **14,** 431-442.

Rolfe KJ, Cambrey AD, Richardson J, Irvine LM, Grobbelaar AO, Linge C (2007). Dermal fibroblasts derived from fetal and postnatal humans exhibit distinct responses to insulin like growth factors. BMC Dev Biol **7,** 124.

Ruetze M, Knauer T, Gallinat S, Wenck H, Achterberg V, Maerz A, Deppert W, Knott A (2013). A novel niche for skin derived precursors in non-follicular skin. J Dermatol Sci **69,** 132-139.

Santini R, Vinci MC, Pandolfi S, Penachioni JY, Montagnani V, Olivito B, Gattai R, Pimpinelli N, Gerlini G, Borgognoni L, Stecca B (2012). Hedgeho-GLI signaling drives self-Renewal and tumorigenicity of human melanoma-initiating cells. Stem Cells **30,** 1808-1818.

Sato N, Meijer L, Skaltsounis L, Greengard P, Brivanlou AH (2004). Maintenance of pluripotency in human and mouse embryonic stem cells through activation of Wnt signaling by a pharmacological GSK-3-specific inhibitor. Nature Medicine **10,** 55-63.

Sato R, Semba T, Saya H, Arima Y (2016). Concise review: stem cells and epithelial-mesenchymal transition in cancer: biological implications and therapeutic targets. Stem Cells **34,** 1997-2007.

Schmole AC, Hubner R, Beller M, Rolfs A, Frech MJ (2013). Small molecules in stem cell research. Curr Pharm Biotechno **14,** 36-45.

Schneider DJ, Wu MH, Le TT, Cho SH, Brenner MB, Blackburn MR, Agarwal SK (2012). Cadherin-11 contributes to pulmonary fibrosis: potential role in TGF-beta production and epithelial to mesenchymal transition. Faseb J **26,** 503-512.

Schneider JW, Gao Z, Li S, Farooqi M, Tang TS, Bezprozvanny I, Frantz DE, Hsieh J (2008). Small-molecule activation of neuronal cell fate. Nat Chem Biol **4,** 408-410.

Shi H, Zhang T, Qiang L, Man L, Shen Y, Ding F (2013). Mesenspheres of neural crest-derived cells enriched from bone marrow stromal cell subpopulation. Neurosci Lett **532,** 70-75.

Shi Y, Do JT, Desponts C, Hahm HS, Scholer HR, Ding S (2008). A combined chemical and genetic approach for the generation of induced pluripotent stem cells. Cell Stem Cell **2,** 525-528.

Shim JH, Lee TR, Shin DW (2013a). Novel in vitro culture condition improves the stemness of human dermal stem/progenitor cells. Mol Cells **36,** 556-563.

Shim JH, Park JY, Lee MG, Kang HH, Lee TR, Shin DW (2013b). Human dermal stem/progenitor cell-derived conditioned medium ameliorates ultraviolet a-induced damage of normal human dermal fibroblasts. PLoS One **8,** e67604.

Stanton BZ, Peng LF, Maloof N, Nakai K, Wang X, Duffner JL, Taveras KM, Hyman JM, Lee SW, Koehler AN, Chen JK, Fox JL, Mandinova A, Schreiber SL (2009). A small molecule that binds Hedgehog and blocks its signaling in human cells. Nat Chem Biol **5,** 154-156.

Su X, Paris M, Gi YJ, Tsai KY, Cho MS, Lin YL, Biernaskie JA, Sinha S, Prives C, Pevny LH, Miller FD, Flores ER (2009). TAp63 prevents premature aging by promoting adult stem cell maintenance. Cell Stem Cell **5,** 64-75.

Suflita MT, Pfaltzgraff ER, Mundell NA, Pevny LH, Labosky PA (2013). Ground-state transcriptional requirements for skin-derived precursors. Stem Cells Dev **22,** 1779-1788.

Suslov ON, Kukekov VG, Ignatova TN, Steindler DA (2002). Neural stem cell heterogeneity demonstrated by molecular phenotyping of clonal neurospheres. P Natl Acad Sci USA **99,** 14506-14511.

Toma JG, Akhavan M, Fernandes KJL, Barnabe-Heider F, Sadikot A, Kaplan DR, Miller FD (2001). Isolation of multipotent adult stem cells from the dermis of mammalian skin. Nat Cell Biol **3,** 778-784.

Toma JG, McKenzie IA, Bagli D, Miller FD (2005). Isolation and characterization of multipotent skin-derived precursors from human skin. Stem Cells **23,** 727-737.

Tseropoulos G, Moghadasi Boroujeni S, Bajpai VK, Lei P, Andreadis ST (2018). Derivation of neural crest stem cells from human epidermal keratinocytes requires FGF-2, IGF-1, and inhibition of TGF-beta1. Bioeng Transl Med **3,** 256-264.

Valastyan S, Weinberg RA (2011). Tumor metastasis: molecular insights and evolving paradigms. Cell **147,** 275-292.

Wang Q, Zhang F, Hong Y (2018). Blocking of autocrine IGF-1 reduces viability of human umbilical cord mesenchymal stem cells via inhibition of the Akt/Gsk-3beta signaling pathway. Mol Med Rep **17,** 4681-4687.

Wei SC, Fattet L, Tsai JH, Guo YR, Pai VH, Majeski HE, Chen AC, Sah RL, Taylor SS, Engler AJ, Yang J (2015). Matrix stiffness drives epithelial mesenchymal transition and tumour metastasis through a TWIST1-G3BP2 mechanotransduction pathway. Nat Cell Biol **17,** 678-U306.

Wenzel V, Roedl D, Gabriel D, Gordon LB, Herlyn M, Schneider R, Ring J, Djabali K (2012). Naive adult stem cells from patients with Hutchinson-Gilford progeria syndrome express low levels of progerin in vivo. Biol Open **1,** 516-526.

Williamson AJ, Doscas ME, Ye J, Heiden KB, Xing M, Li Y, Prinz RA, Xu X (2016). The sonic hedgehog signaling pathway stimulates anaplastic thyroid

cancer cell motility and invasiveness by activating Akt and c-Met. Oncotarget **7,** 10472-10485.

Wu SM, Choo AB, Yap MG, Chan KK (2010). Role of Sonic hedgehog signaling and the expression of its components in human embryonic stem cells. Stem Cell Res **4,** 38-49.

Xiao L, Yuan X, Sharkis SJ (2006). Activin A maintains self-renewal and regulates fibroblast growth factor, Wnt, and bone morphogenic protein pathways in human embryonic stem cells. Stem Cells **24,** 1476-1486.

Xu Y, Zhu XW, Hahm HS, Wei WG, Hao EG, Hayek A, Ding S (2010). Revealing a core signaling regulatory mechanism for pluripotent stem cell survival and self-renewal by small molecules. P Natl Acad Sci USA **107,** 8129-8134.

Yao C, Su L, Shan J, Zhu C, Liu L, Liu C, Xu Y, Yang Z, Bian X, Shao J, Li J, Lai M, Shen J, Qian C (2016). IGF/STAT3/NANOG/Slug signaling axis simultaneously controls epithelial-mesenchymal transition and stemness maintenance in colorectal cancer. Stem Cells **34,** 820-831.

Ying QL, Wray J, Nichols J, Batlle-Morera L, Doble B, Woodgett J, Cohen P, Smith A (2008). The ground state of embryonic stem cell self-renewal. Nature **453,** 519-U515.

Yoshikawa K, Naitoh M, Kubota H, Ishiko T, Aya R, Yamawaki S, Suzuki S (2013). Multipotent stem cells are effectively collected from adult human cheek skin. Biochem Bioph Res Co **431,** 104-110.

Yoshino T, Saito D, Atsuta Y, Uchiyama C, Ueda S, Sekiguchi K, Takahashi Y (2014). Interepithelial signaling with nephric duct is required for the formation of overlying coelomic epithelial cell sheet. P Natl Acad Sci USA **111,** 6660-6665.

Youssef A, Aboalola D, Han VK (2017). The roles of insulin-Llike growth factors in mesenchymal stem cell niche. Stem Cells Int **2017,** 9453108.

Zhang C, Wang Y, Feng Y, Zhang Y, Ji B, Wang S, Sun Y, Zhu C, Zhang D, Sun Y (2016). Gli1 promotes colorectal cancer metastasis in a Foxm1-dependent manner by activating EMT and PI3K-AKT signaling. Oncotarget **7,** 86134-86147.

Zhang K, Sun CP, Zhang Q, Wang XJ (2015). Sonic hedgehog-Gli1 signals promote epithelial-mesenchymal transition in ovarian cancer by mediating PI3K/AKT pathway. Medical Oncology **32**, 368.

Zhao MT, Whitworth KM, Lin H, Zhang X, Isom SC, Dobbs KB, Bauer B, Zhang Y, Prather RS (2010). Porcine skin-derived progenitor (SKP) spheres and neurospheres: Distinct "stemness" identified by microarray analysis. Cell Reprogram **12,** 329-345.

Zhong JL, Edwards GP, Raval C, Li H, Tyrrell RM (2010). The role of Nrf2 in ultraviolet A mediated heme oxygenase 1 induction in human skin fibroblasts. Photochem Photobiol Sci **9,** 18-24.

Zhou J, Zhu G, Huang J, Li L, Du Y, Gao Y, Wu D, Wang X, Hsieh JT, He D, Wu K (2016). Non-canonical GLI1/2 activation by PI3K/AKT signaling in

renal cell carcinoma: A novel potential therapeutic target. Cancer Lett **370,** 313-323.

국문초록

Sonic hedgehog 신호조절 소분자물질 및 인슐린유사성장인자1이 마우스 피부유래전구세포 형성에 미치는 효과

박 상 규

서울대학교 대학원

치의과학과 종양및발달생물학 전공

(지도교수: 노상호)

피부유래전구세포는 중간엽줄기세포 및 신경능선세포의 특성을 가지고 있는 세포로서 지방, 골, 연골 및 신경세포로의 분화가 가능하다. 따라서, 피부유래전구세포는 두개악안면을 형성하는 신경능선줄기세포의 특성을 갖고 있으므로 치의학 연구에서 중요한 세포자원이다. 이러한 피부유래전구세포는 전체 피부세포에서 적은 군집을 가지고 있기 때문에 세포를 얻기가 어렵다. 따라서 본 연구는 마우스 피부로부터 유래된 피부유래전구세포의 특성을

파악하고, 증식에 영향을 미치는 신호전달경로를 규명하여 증식력을 높이는데 그 의의가 있다. 실험을 위해 태령 16.5일에서 17.5일경 마우스의 등 쪽 피부로부터 분리된 조직에서 단일세포를 분리하고, 피부유래전구세포 배양액 (EGF, FGF2, B27이 포함된 F12/DMEM)에서 부유배양을 통해 구형의 피부유래전구세포를 획득하였다. 이렇게 획득된 구형세포는 그 특징을 확인하기 위해 지방, 골, 신경세포로의 분화를 유도하였다. 마우스 피부유래전구세포는 단일세포로부터 구형세포로 형성이 되었고, 지방, 골, 신경세포의 분화를 확인하였다. 확립된 피부유래전구세포를 활용하여 신호전달경로 활성화 및 억제 효과를 증식력, 유전자 분석, 단백질 분석과 면역형광법을 통해 각각 분석하였고, 이와 같은 결과는 통계적 처리법을 통해 유의적인 차이를 확인하였다. 첫번째 연구는 피부전구세포의 증식에 영향을 미칠 것으로 예상되는 다양한 신호전달경로 중에서, 특히 발달과정에서 중요하게 작용하는 Sonic hedgehog (Shh) 신호 경로를 활성화 또는 억제하는 소분자물질의 처리를 통해 Shh 신호 경로가 피부유래전구세포에 미치는 영향을 확인하였다. 우선, 재조합 Shh 성장인자를 처리하여 증식효과를 확인하였으며, 구형의 피부유래전구세포에는 Shh 신호전달경로 작용물질인 Purmorphamine (Pur), 길항물질인 Cyclopamine (CP),

Gli 길항물질인 GANT-61 같은 소분자물질을 처리하여 Shh-Gli1 신호 경로를 활성화 또는 억제하여 영향을 확인하였다. 그 결과, Pur의 처리에 의한 Shh 신호경로의 활성화는 피부유래전구세포의 증식력을 높였고, CP의 처리에 의해 Shh 신호경로가 억제 시 구형세포의 형성 및 증식력이 감소되는 것을 확인하였다. GANT-61 처리에 의해 Gli1을 억제하였을 때 역시 증식력과 구형세포가 감소함을 확인하여 피부유래전구세포에서 Shh 신호경로는 증식하는데 중요한 메커니즘임을 확인하였다. 두번째 연구는, 신경줄기세포의 구형세포의 형성에 중요하게 작용하는 인슐린유사성장인자1을 처리하여 증식에 미치는 효과를 확인하였다. 인슐린유사성장인자1의 처리에 의해 구형세포가 커지고 세포의 증식력이 향상되는 것을 확인하였고, 과산화수소의 처리를 통해 억제된 증식력을 인슐린유사성장인자1이 회복시키는 것을 확인하였다. 특히, 활성산소를 감소시키고, 산화적 스트레스 저항 마커의 발현을 증가시켰다.

본 연구결과는 피부유래전구세포의 증식과 구형세포를 형성하는 자가복제관련 분자기작을 이해하고, Shh-Gli 신호경로가 이러한 피부유래전구세포의 자가복제와 증식을 증진시킬 수 있음을 확인하였다. 또한, 인슐린유사성장인자1은 피부유래전구세포의 증식

및 활성산소의 억제에 효과적으로 작용함을 확인하였다. 이와 같은 연구결과는 피부유래전구세포의 증식기전을 이해하고, Shh와 인슐린유사성장인자1의 신호전달경로 활성화 유도에 의한 피부전구세포의 형성 촉진에 기여하여 치료에 적합한 세포를 대량 획득할 수 있을 것으로 기대된다.

주요어 : Sonic hedgehog, 피부유래전구세포, 증식, 줄기세포, Shh, 소분자물질, 인슐린유사성장인자 1, 자가복제

학 번 : 2007-23382